Yi-Balan, S. A., Amundson, R., & Buss, H. L. (2014). Decoupling of sulfur and nitrogen cycling due to biotic processes in a tropical rainforest. *Geochimica et Cosmochimica Acta*, *142*, 411-428. https://doi.org/10.1016/j.gca.2014.05.049

Decoupling of sulfur and nitrogen cycling due to biotic processes in a tropical rainforest

Simona A. Yi-Balan[a,*], Ronald Amundson[a], Heather L. Buss[b]

[a]*Department of Environmental Science, Policy and Management, 140 Mulford Hall, University of California, Berkeley, CA 94720, USA*

[b]*School of Earth Sciences, University of Bristol, Bristol BS8 1RJ, UK*

Abstract

We examined the terrestrial sulfur (S) cycle in the wet tropical Luquillo Experimental Forest (LEF), Puerto Rico. In two previously instrumented watersheds (Icacos and Bisley), chemical and isotopic measurements of carbon (C), nitrogen (N) and S were used to explore the inputs, in-soil processing, and losses of S through comparison to the N cycle. Additionally, the impact of soil forming factors (particularly climate, organisms, topography and parent material) on S cycling in this system was considered. Atmospheric inputs (δ^{34}S values of 16.1±2.8‰), from a mixture of marine and anthropogenic sources, delivered an estimated 2.2 g S/(m^2yr) at Icacos, and 1.8 g S/(m^2yr) at Bisley. Bedrock N and S inputs to soil were minimal. We estimated a hydrologic export of 1.7±0.1 g S/(m^2yr) at Icacos, and 2.5±0.2 g S/(m^2yr) at Bisley. Stream

* Corresponding author.
Phone number: (+1) 510-725-2420
E-mail address: sbalan@berkeley.edu (S. Yi-Balan)

baseflow S isotope data revealed significant bedrock S in the hydrologic export at Bisley (with a distinctive $\delta^{34}S$ values of 1.6±0.7‰), but not at Icacos. Pore water data supported the co-occurrence of at least three major biological S-fractionating processes in these soils: plant uptake, oxidative degradation of organic S and bacterial sulfate reduction. The rates and relative importance of these processes varied in time and space. Vegetation litter was 3 to 5‰ depleted in ^{34}S compared to the average pore water, providing evidence for fractionation during uptake and assimilation. Out of all abiotic soil forming factors, climate, especially the high rainfall, was the main driver of S biogeochemistry in the LEF by dictating the types and rates of processes. Topography appeared to impact S cycling by influencing redox conditions: C, N and S content decrease downslope at all sites, and the Bisley lower slope showed strongest evidence of bacterial sulfate reduction. Parent material type did not impact the soil S cycle significantly. To compare the fate of S and N in the soil, we used an advection model to describe the isotopic fractionation of total S and N associated with downward movement of organic matter in both dissolved and solid fractions. This model worked well for N, but the assumption of a constant fractionation factor α with depth failed to describe S transformations. This result revealed a fundamental difference between N and S cycling in these soils, indicating an apparent greater sensitivity of S isotopes to fluctuating redox conditions.

Abbreviations

COS: carbonyl sulfide

CZO: Critical Zone Observatory

DMS: dimethyl sulfide

DOS: dissolved organic sulfur

LEF: Luquillo Experimental Forest

LTER: Long-Term Ecological Research

MAP: mean annual precipitation

masl: meters above sea level

MAT: mean annual temperature

MSA: methanesulfonic acid

NAD83: North American Datum of 1983

NRCS: National Resources Conservation Service

nss: non-seasalt

SOS: soil organic sulfur

USDA: United States Department of Agriculture

USGS: United States Geologic Survey

1. INTRODUCTION

The terrestrial biogeochemical cycle of an element is driven by inputs, outputs, and transformations within the plant/soil system (e.g. Vitousek and Stanford, 1986). Sulfur (S), like nitrogen (N), has a complex biogeochemical cycle for two main reasons. First, S exists in a wide range of valence states (from -2 to +6), and can participate in intricate biochemical reactions, some of which are challenging to elucidate (Norman et al., 2002; Brunner and Bernasconi, 2005; Bradley et al., 2011; Sim et al., 2011). Second, S is an essential nutrient, but soils can suffer both from S deficiency (Acquaye and Beringer, 1989; Tabatabai, 1984), and from S excess (via pollution, or naturally sulfide-rich bedrocks) (Likens et al., 2002). Unlike N however, for which both the natural and the human-impacted cycles have been well studied, S has been studied mostly in industrialized regions subject to high deposition rates (e.g. Novak et al., 2001; Likens et al., 2002; Marty et al., 2011), and we still lack a basic understanding of the natural controls on the S cycle in less perturbed environments. Based on N studies (e.g. Austin and Vitousek, 1998; Amundson et al., 2003), it is likely that the soil formation factors identified by Jenny (1941) (climate, organisms, topography, parent material and time) play a role in the soil S cycle, however no previous research has addressed these controls systematically.

A potential impact of topography was observed in Costa Rica, where Bern and Townsend (2008) found that hillslope soils had higher $\delta^{34}S$ values compared to alluvial soils. Climate should have a first order impact on redox-sensitive elements, as mean annual precipitation (MAP) impacts elemental input and loss rates, and the dominant biological processes in the soil, while mean annual temperature (MAT) impacts the rates of biotic processes such as bacterial sulfate reduction (Bruchert et al., 2001; Canfield et al., 2006; Turchyn et al., 2010). Previous research found that wet tropical forest soils may emit hydrogen sulfide due to dissimilatory sulfate

reduction (Delmas and Servant, 1983; Delmas et al., 1978; Newman et al., 1991), however this was shown not to be an important process in Costa Rica, where most of the S research on pristine wet tropical forest soils to date has focused (Bern et al., 2007; Bern and Townsend, 2008). Hillslope soils in Costa Rica depend exclusively on atmospheric S inputs, show minimal variation in concentration and isotope values with depth, and an overall slight enrichment in ^{34}S compared to the precipitation. This isotopic enrichment may be due to emissions of highly depleted biogenic S gases by vegetation, or due to oxidative degradation of organic S (Bern et al., 2007; Bern and Townsend, 2008). Fractionation during plant uptake is negligible (Bern and Townsend, 2008). The largest S isotope fractionations observed in nature occur during microbial dissimilatory sulfate reduction, which can deplete the sulfide products by up to 70‰ (Brunner and Bernasconi, 2005). Despite their generally small magnitude (Table A1), other biological fractionations sensitive to climate are also significant because they all operate in the same direction: microbes and plants preferentially utilize the lighter isotope during metabolism, therefore $\delta^{34}S$ values tend to decrease in products compared to the substrates (see Table A2 for a compilation of input $\delta^{34}S$ values). An overview of the soil S cycle, based on current knowledge, is illustrated in Fig. A1.

Here we use stable isotopes to investigate the geochemical cycling of S in the wet montane forest ecosystem of the Luquillo Experimental Forest (LEF) in Puerto Rico, and compare it to the better-known N cycle. At the LEF, previous studies have focused on rates of chemical weathering and solute loss (e.g. White et al., 1998; Murphy et al., 1998; Schulz et al., 1999; Buss et al., 2008), and on the sources and cycling of nutrients such as N and P (e.g. Silver et al., 1994; Pett-Ridge et al., 2009; Buss et al., 2010). Sulfate and/or total S concentrations have been measured in precipitation (McDowell et al., 1990; Asbury et al., 1994; White et al., 1998;

Heartsill-Scalley et al., 2007), soil and saprolite (Cox et al., 2002; White et al., 1998; Stanko-Golden and Fitzgerald, 1991), and major streams (White et al., 1998; McDowell and Asbury, 1994; Bhatt and McDowell, 2007). Here we integrate and expand on these previous studies and present novel stable S and N isotope data for the coupled precipitation-soil-vegetation system, to address two yet unanswered questions: (1) how do soil forming factors, particularly bedrock and topography, impact S biogeochemistry in a tropical environment? and (2) are the N and S biogeochemical cycles coupled, or at least similar, in tropical soils? These questions have importance for understanding spatial patterns of nutrient dynamics and feedbacks, and for setting a baseline for studying the response of tropical soils to climate or land use change.

2. SITE DESCRIPTION

The Luquillo Experimental Forest (LEF) (18°18'N, 65°50'W, referenced to the NAD83 datum) is a Long-Term Ecological Research (LTER) and Critical Zone Observatory (CZO) site, with a long history of biogeochemical research (e.g. Scatena, 1989; McDowell et al., 1990; Silver et al., 1994; White et al., 1998). MAP in this warm and humid tropical forest increases with elevation, ranging from about 2500 mm to over 5000 mm at the highest elevation of 1074 m (Scatena, 1989; McDowell and Asbury, 1994). Rainfall is significant year round, with January through April being the driest period (Heartsill-Scalley et al., 2007). Precipitation occurs mostly as frequent, short, high intensity events (White et al., 1998; Scatena, 1989; Buss et al., 2010). Convective boundary layer storms with strong orographic effects are most common (White et al., 1998), but northeasterly trade winds, winter cold fronts, tropical storms, depressions and hurricanes also affect the region (Heartsill-Scalley et al., 2007). MAT is 22-23°C at both sites (White et al., 1998; Murphy and Stallard, 2012).

Our study focused on two LEF watersheds instrumented by the USGS (White et al., 1998; Buss et al., 2011; Buss and White, 2012): Icacos (mature Colorado forest on quartz diorite) and Bisley (mature Tabonuco forest on volcaniclastics) (Fig. 1). The Icacos site is located on the shoulder of the Guaba ridge in the catchment of the Guaba stream, a tributary of Rio Icacos (see White et al., 1998, for a detailed description of the site). The site is above the average cloud condensation level at 600 m (Cox et al., 2002). Icacos soils are a somewhat poorly drained mix of Ultisols (Boccheciamp, 1977) and Inceptisols (Huffaker, 2002; Soil Survey Staff, Web Soil Survey). The profile we investigated was a Plinthic Haplohumult, closely matching the Los Guineos series (very fine, kaolinitic, isothermic Humic Haplodox). The Bisley site is located within the Rio Mameyes drainage system (Scatena, 1989), at an elevation below the average cloud condensation level. Soils are well drained on convex slopes, and somewhat poorly drained on concave slopes (Murphy et al., 2012). The soils are mapped as clay-rich Ultisols (Scatena, 1989; Johnston, 1992; Cox, et al, 2002; Soil Survey Staff, Web Soil Survey). The profile we investigated was a Typic Haplohumult, corresponding to the Humatus series.

Each site has soil water and gas samplers augered in a transect from a hillslope nose downslope to the adjacent stream channel – a toposequence. In 1992, at Icacos, White et al. (1998) installed ceramic cup suction lysimeters at three topographic locations on the Guaba Ridge: local ridgetop, steep hillslope (~50% grade, downhill from the ridgetop) and ridge shoulder (moderate slope, ~25% grade, uphill from the local ridgetop) – sites LG-1, LG-2 and LG-3, respectively. At Bisley, Buss et al. (2011) developed a similar installation on a ridgetop, upper slope and lower slope (riparian) (sites B1S1, B1S2 and B1S4 respectively). The approximate coordinates for the Icacos and Bisley lysimeter fields (referenced to the NAD83) are N18°16.9', W65°47.4' and N18°18.9', W65°44.7' respectively. Additionally, ground water wells were installed at both sites

149 (coordinates: N18°16.94', W56°47.34' at Icacos, N18°18.93', W65°44.75' at Bisley, WGS84
150 datum; Buss and White, 2012). The two sites have similar S deposition chemistry.

151

152 **3. METHODS**

153 **3.1 Sample collection**

154 Field investigations followed standard field methods (Schoeneberger et al., 2002). At the highest
155 topographic position, trenches were excavated to 2 m and sampled by horizon. At all hillslope
156 positions, two 1.5 m-deep hand-augered cores and fresh leaf litter from the forest floor were
157 collected. During the initial field campaign in June 2010, all operational lysimeters were
158 sampled. Subsequently, four lysimeters in the upper 2 m of the soil at each subsite were sampled
159 monthly from February 2011 until February 2012, whenever water was present. The aim was to
160 collect water at 15, 60, 150 and 180 cm; however, if functional lysimeters were unavailable at
161 those depths at a site, we used the closest functional ones instead (Table A3).

162 Precipitation (openfall) was sampled monthly from June 2010 to March 2012, and then again in
163 June 2012, at a station 2 km east of the Icacos site on Pico del Este (elevation 1051 m, MAP
164 4436 mm averaged over the period 1970-1994; Garcia-Martino et al. 1996). The collectors were
165 emptied weekly, thus each sample is the average deposition for the preceding week. This method
166 of collecting openfall reflects rainfall plus the coarse particulate fraction that settles out via
167 gravity (McDowell et al., 1990), but not the more abundant fine particulate and gaseous fraction
168 scavenged by the forest canopy.
169 Baseflow stream water was collected from the Guaba and Bisley streams in February, March and
170 June 2012, and a groundwater sample was collected in August 2012 at a depth of ~6.1 m from a

well at the Icacos site. It was not possible to retrieve enough water for isotope analyses from a well at Bisley (9.6 m deep).

3.2 Sample processing and analysis

Soils were stored at room temperature in sealed bags. For total soil S isotope and chemical analysis, splits of the samples were dried at 60°C overnight, sieved to <2 mm, and ground with a mortar and pestle. Plant-available sulfate was extracted from splits of unprocessed samples by shaking for a minimum of 4 hours in a 1:7 soil to deionized water mixture, centrifuging for 30 minutes at 3000 rpm, and then filtering the supernatant to 0.7 µm glass microfiber filters. Litter samples were kept frozen then freeze-dried and pulverized in a ball mill.

Rain and pore water samples were shipped frozen from Puerto Rico to Berkeley, then filtered in the lab to 0.7 µm within a few days of sampling, and stored refrigerated until further use. Only water samples with a volume greater than 500 ml were processed for isotope measurements to ensure sufficient quantities of sulfate. For sulfate isotope analysis, filtered water samples were heated in a warm water bath, and a 1M $BaCl_2$ solution was added in excess (in a quantity equal to approximately 10% of the sample volume). After 24 hours, the samples were acidified with a few drops of 1N HCl to dissolve carbonates, then filtered again on a 1.6 µm filter to collect the $BaSO_4$ precipitate. Because the samples were low in S, it was impossible to remove the $BaSO_4$ precipitate, therefore the entire surface of the filter was scraped off for combustion in the elemental analyzer/mass spectrometer. The S content of blank filter samples was below the detection limit.

192 The anion content of the soil extracts and water samples was determined on a Dionex ICS-1500
193 ion chromatograph with an IonPac AS9-HC 4 mm column, a 9 mM sodium bicarbonate eluent at
194 a flow rate of 1.0 mL/min and an international seven anion standard from Dionex. The analytical
195 precision of the instrument, in the range of values measured, was +/-10%.

196 The C and N contents (% dry weight) and stable isotope ratios ($\delta^{13}C$ and $\delta^{15}N$) of soil and litter
197 samples were determined via elemental analyzer/continuous flow isotope ratio mass
198 spectrometry using a CHNOS Elemental Analyzer (Vario ISOTOPE Cube, Elementar, Hanau,
199 Germany) coupled with an IsoPrime100 IRMS (Isoprime, Cheadle, UK) at the Center for Stable
200 Isotope Biogeochemistry, University of California, Berkeley. The reference material NIST SMR
201 1547 (peach leaves) was used as a calibration standard. Long-term external precision for C and N
202 isotope analyses was 0.10‰ and 0.15‰, respectively.

203 The total S concentration and $\delta^{34}S$ values of soils and litter, and the $\delta^{34}S$ value of sulfate in water
204 samples, were determined using the SO_2 EA-combustion-IRMS method on a GV Isoprime
205 isotope ratio mass spectrometer coupled with an Eurovector Elemental Analyzer (model
206 EuroEA3028-HT) at the Laboratory for Environmental and Sedimentary Isotope Geochemistry
207 (LESIG), University of California at Berkeley. Briefly, a small amount of powdered sample
208 containing a minimum of 2 μg S mixed with V_2O_5 catalyst was thermochemically decomposed
209 with copper wires at 1020°C, and the isotopic composition of the resulting SO_2 gas was
210 measured. Water vapor was removed with a $Mg(ClO_4)_2$ trap and CO_2 was eluted out using a
211 dilutor. Several replicates of the international standard NBS127 and two lab standards (both pure
212 $BaSO_4$) were run with each batch of samples. The long-term analytical precision of this method
213 is better than 0.2‰.

Due to the lack of certified soil and organic material standards for S isotope analyses, we selected several different material types and cross-validated the results from the LESIG lab against measurements from other labs. The results, displayed in Table A4, show that the averages obtained by this lab agree well with those from other labs, and with good precision.

3.3 Models and calculations

The isotope composition is reported using standard δ notation:

$$\delta(‰) = \left(\frac{R_{Sample}}{R_{Standard}} - 1\right) \cdot 1000, \quad (1)$$

where R is the ratio of the rare to the common isotope. For $\delta^{34}S$, R is the ratio of ^{34}S to ^{32}S and the standard is Canyon Diablo Troilite (CDT). Isotope fractionation can be described by the fractionation factor α:

$$\alpha = \frac{R_{Product}}{R_{Substrate}}, \quad (2)$$

the enrichment factor ε:

$$\varepsilon = (\alpha - 1) \cdot 1000 \quad (2)$$

and the Δ value:

$$\Delta = \delta_{Product} - \delta_{Substrate} \cong 1000 \cdot ln\frac{R_{Product}}{R_{Substrate}}. \quad (4)$$

Following other studies (e.g. Brenner, 1999; Baisden et al., 2002; Sanderman and Amundson, 2008), we examined the content and isotopic composition of organic matter with depth, assuming that its transport occurs through largely advective processes (i.e. vertical transport of a

233 solute or particulate matter in the liquid phase), and that during transport, decomposition creates
234 aqueous or gaseous products that leave the system. At steady state, in soils where aboveground
235 inputs far exceed belowground inputs, the advection/decomposition equations for the abundant
236 and rare isotopes are (after Brenner, 1999):

237 $$\frac{\delta[^{32}S]}{\delta t} = 0 = \upsilon \frac{\delta[^{32}S]}{\delta z} - k^{32}S \quad (5)$$

238 $$\frac{\delta[^{34}S]}{\delta t} = 0 = \upsilon \frac{\delta[^{34}S]}{\delta z} - k\alpha^{34}S \quad (6)$$

239 where ν is the advection coefficient (in cm/yr), k is the first order organic matter decay constant
240 (in yr^{-1}) and α is the fractionation factor. In terms of the heavy to light isotope ratio R, the
241 general solution becomes:

242 $$\frac{R(z)}{R(0)} = e^{-\frac{kz}{\upsilon}(\alpha-1)} \quad (7)$$

243 where R(z) and R(0) are the $^{34}S/^{32}S$ ratios of the soil at depth z and of the inputs respectively.
244 Denoting the fraction of total S remaining at depth z compared to the surface inputs as *f*:

245 $$\frac{S(z)}{S(0)} = e^{-\frac{kz}{\upsilon}} = f \quad (8)$$

246 we can rewrite Eqn. 7 as:

247 $$\frac{R(z)}{R(0)} = f^{(\alpha-1)} \quad (9)$$

248 In δ notation, Eqn. 9 is equivalent to:

249 $$\delta(z) = \varepsilon \cdot lnf + \delta(0) \quad (10)$$

Furthermore, at fractionation factors α close to unity, Eqn. 9 converts to (Ewing et al., 2008; Amundson et al., 2012):

$$\delta(z) = (\delta_i(z) + 1000) \cdot f(z)^{(\alpha-1)} - 1000 \quad (11)$$

To model this for N and S, we assigned the parameters as follows: $\delta(z=0)$ equals the $\delta^{15}N$ or $\delta^{34}S$ value of the A horizon; for any subsequent horizons, $\delta_i(z) = \delta(z-1)$; and $f(z)$ equals the ratio of total soil N or S at depth z to the total soil N or S content of the uppermost horizon. We calculated the α values that best fit the data.

We calculated any S contributed to pore water by rock weathering as the amount measured in pore water minus the amount contributed by rainfall corrected for evapotranspiration (after White et al., 2009):

$$S_{weathering} = S_{pore\ water} - S_{rainfall}\left[\frac{Cl_{pore\ water}}{Cl_{rainfall}}\right] \quad (12)$$

We calculated the sulfate flux Q through the regolith (soil+saprolite) with the equation:

$$Q = q_h \Delta c \quad (13)$$

where q_h is the vertical infiltration rate or field flux density (product of the hydraulic conductivity and the hydraulic gradient), and $\Delta c = c_f - c_i$ is the change in concentration between two depths (White et al., 1998). White et al. (1998) reported a vertical infiltration rate of 1 m/yr at Icacos. Here we used the hydraulic field flux density values from Buss et al. (2011), which are corrected for evapotranspiration: 1.28 m/yr at Icacos and 1.62 m/yr at Bisley. Sulfate fluxes were calculated to and from a given depth interval by multiplying q_h times the difference in the average sulfate concentration between the lysimeter sampled at that depth (c_f) and the one

directly above it (c_i). For the topmost lysimeters, the starting concentration c_i is the sulfate concentration in precipitation. The isotopic enrichment associated with additions or losses in pore water was expressed as the difference between the $\delta^{34}S$ value of the two lysimeter samples (i.e. the Δ value, Eqn. 4)

4. RESULTS

4.1 Field observations

Both excavated soil profiles, located at the highest topographic location of each transect, had high clay contents, reddening and loss of rock structure (Table 1). The granitic soil at Icacos had about 5% less clay than the volcanic-derived soil at Bisley. In addition, the clay content of the Icacos soil sharply declined below 111 cm, whereas it remained high to the depth of excavation (158 cm) at Bisley. In the upper 16-17 cm, both soils were rich in humus and highly mixed by earthworms. Below 17 cm, significantly darker patches or zones in the soil profile suggest that humus had also accumulated in some subsurface horizons. Below the well-mixed biotic horizons, clay content increased and the soil color indicated gleying, suggesting at least periodic reducing conditions. The Icacos soil had a prominent zone of plinthite (red areas enriched in Fe (III) oxide adjacent to gray, Fe (III)-depleted zones, formed in response to fluctuating water tables and redox conditions) above a 10 cm-thick layer displaying Mn oxide stains. In general, both soils showed evidence of reducing conditions due to periodic saturation, and adequate C for microbial metabolism and oxygen consumption.

4.2 Vegetation litter and soil chemistry

C, N and S contents and stable isotope values vary widely among vegetation types (Table 2). Palo Colorado (*Cyrilla racemiflora*, the dominant tree at Icacos) leaves have a C:N ratio twice that of Tabonuco (*Dacryodes excelsa*, the dominant tree at Bisley) leaves (54:1 versus 27:1), higher C:S (308:1 versus 253:1), but lower N:S (6:1 versus 9:1) (Table 2). The difference is even more pronounced in the O horizon (C:N ratio of 78:1 at Icacos versus 29:1 at Bisley, C:S ratio 522:1 versus 317:1, and N:S ratio 7:1 versus 11:1). As expected, mineral soil C and N content declines exponentially with depth at all sites. C and N content also decreases downslope, with highest values on the ridges (surface values of 3.99±0.20% C and 0.22±0.01% N at Icacos, and 4.31±0.22% C and 0.35±0.02% N at Bisley). Total soil S and water extractable sulfate (Fig. 2) concentrations are highest in the surface horizons. Sulfate declines exponentially with depth, to <1 mg S/kg. In contrast, total S – largely in organic forms – decreases irregularly with soil depth, and has subsurface accumulations that correspond to the visual humus increases in some clay-rich horizons. The mineral soil has a lower S content than the O horizon. Total soil S content (in mg/kg) is highest on ridgetops in the top 10 cm, but decreases downslope when averaged over the upper meter. The highest S concentrations occur in the Bisley ridgetop soil (625±27 mg S/kg in surface samples and 346±7 at the bottom of the profile), and the lowest in the Bisley lower slope soil (189±16 mg/kg at the surface, 12±3 mg/kg at the bottom). C:S ratios decrease nearly exponentially with depth, from 130:1 to 3:1 at Icacos, and from 81:1 to 4:1 at Bisley (Fig. 2). The decrease is less pronounced in the Bisley lower slope site. Similarly, N:S ratios generally decrease with depth from 7.2:1 to 0.1:1 at Icacos, and from 9.2:1 to 0.5:1 at Bisley. N:S ratios are highest throughout at the Bisley lower slope site, and remain relatively constant with depth.

The $\delta^{13}C$ values of Palo Colorado leaves are slightly higher than those of Tabonuco (-33.2 versus -36.0‰), but the O horizons both have similar $\delta^{13}C$ values (-30‰). Despite higher $\delta^{15}N$ values in

plant litter at Icacos (0.97 compared to -0.51‰), $\delta^{15}N$ values of the O horizon are more negative at Icacos than at Bisley (-1.4 compared to -0.04‰). As expected, soil $\delta^{13}C$ and $\delta^{15}N$ values exceed those in plant litter and the O horizon, and generally increase with depth. Surface (top 10 cm) $\delta^{13}C$ values are independent of topographic position. Surface soil $\delta^{15}N$ values are highest in the Bisley soils, and increase downslope at Bisley (4.56±0.5‰ on the ridgetop, 6.45±0.6‰ on the upper slope and 6.8±0.8‰ on the lower slope), but are unaffected by topographic location at Icacos. The two sites have similar litter (15.4 and 14.9‰) and O horizon (12.9 and 13.3‰) $\delta^{34}S$ values. The mineral soil is enriched in ^{34}S compared to the O horizon (depth-weighted average soil $\delta^{34}S$ values between 13.6 and 18.9‰, depending on the site) (Fig. 2). The difference between the $\delta^{34}S$ values of litter and the top 10 cm of the soil ranges from -2.1 to 1.4‰.

4.3 Water chemistry

The precipitation chemistry data integrate wet and coarse-sized dry inputs to the ecosystem. Total precipitation chemistry varied widely, with sulfate concentrations ranging from 4.6 to 38.8 μM, and $\delta^{34}S$ values from 10.7 to 20.5‰ (Table 3). Precipitation sulfate $\delta^{34}S$ values are uncorrelated with time of the year or sulfate concentration. The volume-weighted average precipitation $\delta^{34}S$ value is 16.1±2.8‰.

The sea salt sulfate was estimated according to:

$$seasalt\ SO_4 = 0.052 \cdot Cl \quad (14)$$

where 0.052 is the sulfate to chloride ratio in seasalt (Keene et al., 1986). Calculations suggest that sea salt contributes 37% of the precipitation sulfate, with a range from 12 to 74%. Conversely, over a quarter of the precipitation sulfate (26-88%) is of non-seasalt origin (Table 3)

– assuming that S is as effectively transported as Cl. Our estimates however refer only to the coarse non-seasalt aerosol fraction, not to the fine aerosol fraction scavenged by the canopy.

The Guaba stream sulfate concentration (14.6±0.5 μM) resembles that of the volume-weighted precipitation average. The sulfate concentration of the Bisley stream (39.4±0.3 μM) is two and a half times greater than that of the Guaba, and just slightly larger than the precipitation maximum. Guaba $\delta^{34}S$ values (19.5±1.6‰) overlap with the precipitation average, and resemble the values of the groundwater (Table 4). On the other hand, the Bisley stream $\delta^{34}S$ (1.6±0.7‰) is much closer to the $\delta^{34}S$ of volcanic or basalt S (see Table A2).

Pore water sulfate concentrations and isotope ratios (Fig. 4) fluctuate with depth and season, though less so at Bisley than at Icacos. Averaged Icacos pore water sulfate concentrations resemble those in groundwater, the Guaba stream, and volume-weighted precipitation averages, except for higher values near the soil surface. The Bisley pore waters also resemble the precipitation average, except for higher sulfate concentrations at 183 cm in the saprolite. All Bisley pore water samples contain significantly less sulfate than the Bisley stream. Average pore water sulfate $\delta^{34}S$ values vary little with depth. The $\delta^{34}S$ values of the Icacos samples exceed the volume-weighted precipitation average, but not the groundwater and baseflow values. The Bisley pore water samples are significantly enriched in the heavy isotope compared to the volume-weighted precipitation average and the Bisley stream. We found no contribution of bedrock S to soils. Relating the pore water S (Fig. 4) and precipitation S and Cl data (Table 3) with Eq. 12 indicates negative weathering S sources (e.g. net loss). Only the saprolite at Bisley (right below the soil zone) revealed between 9 to 44% rock-derived S contributions.

5. DISCUSSION

5.1 The tropical S cycle

Previous work has determined that both sites are likely near quasi-steady state with respect to the biogeochemical cycling of C, N, and S (e.g. Chestnut et al., 1999; Stallard, 2012b). C cycling rate constants have not been determined, but based on MAT, extrapolating from other studies, an organic matter turnover time of ~10 years for the most rapidly cycling pools is likely (Sanderman et al., 2003). As a starting assumption, the S cycle in Puerto Rico is assumed to resemble the one illustrated in Fig. A1. At steady state, the balance between the inputs and losses will determine the $\delta^{34}S$ value of soil S.

5.1.1 S sources to the LEF soils

Previous stream chemistry research (McDowell and Asbury, 1994; Stallard, 2012a) has shown that atmospheric sources provide the bulk of S in this rainforest soil. Our results, based on pore water chemistry, are consistent with this interpretation. Multiplying the MAP times the average sulfate content of rain water (Table 3) suggests an atmospherically-derived S flux of 2.2 g $S/(m^2yr)$ at Icacos, and 1.8 g $S/(m^2yr)$ at Bisley, consistent with the results of McDowell and Asbury (1994) based on stream composition.

At the LEF, atmospherically-derived S has five main potential sources: seasalt, marine non-seasalt sulfate, volcanic ash input, Saharan dust, and anthropogenic emissions. Out of the 16 precipitation samples that were large enough for S isotope measurements, the non-seasalt sulfate $\delta^{34}S$ values ranged between 6.3 and 11.6‰ for 6 samples (Table 3), which is less than the typical

range of 12.5 to 18.7‰ for sulfate produced by DMS oxidation (Calhoun et al., 1991). Three other samples had a total sulfate $\delta^{34}S$ value less than the average of precipitation over the Atlantic Ocean (13.3‰; Chukrov et al., 1980). The fact that seasalt and DMS fail to fully account for the total S indicates significant non-marine sources at certain times of the year.

Volcanic sources of sulfate (average $\delta^{34}S$ of 5‰) are unlikely given that the closest active volcano is Soufrière Hills on the Island of Montserrat (16°45'N, 62°12'W), about 500 km to the southeast, and no significant volcanic activity was reported over the study period. Saharan mineral dust is known to deliver nutrients such as K, Mg (McDowell et al., 1990), Ca (Heartsill-Scalley, et al, 2007) and P (Pett-Ridge, 2009) to the LEF soils. While Saharan dust reaching Puerto Rico does contain measurable sulfate (Reid et al., 2003; Stallard, 2012a), its quantitative importance is unclear. Heartsill-Scalley et al. (2007) found insignificant differences between sulfate fluxes during Saharan dust times (April-September) and the rest of the year at Bisley, concluding that dust contributes minimal sulfate. Here we observed a slight increase in the sulfate concentrations (Table 3) during April-September (volume-weighted average of 16.6 vs. 14.7 μM respectively), and $\delta^{34}S$ values were slightly lower during April-September than the rest of the year (volume-weighted averages of 15.6 and 17.1‰ respectively). The $\delta^{34}S$ value of sulfate from Saharan marine evaporite deposits (17-19‰) is indistinguishable from that of the marine non-seasalt input (Brandmeier et al., 2011). However, Saharan dust collected over the North Atlantic Ocean has lower $\delta^{34}S$ values that range between 11 and 13‰ (Gravenhorst, 1978). To explain this, it has been suggested that the depleted S in Saharan dust is probably not of Saharan soil origin, but rather anthropogenic SO_2 oxidized on the dust (Savoie et al., 1989; Harris et al., 2012), although Saharan soil $\delta^{34}S$ values have not been measured. It is thus possible

that at least some of the precipitation samples reflect inputs of long-range sources of anthropogenic S.

The low $\delta^{34}S$ values of samples collected during winter months (January and March) may also reflect anthropogenic inputs. Anthropogenic S (and N) can reach the LEF from North America via Northern cold fronts (McDowell et al., 1990), which deliver 5% of the rainfall at LEF (Scholl et al., 2009). Northern Hemisphere contaminant deposition peaks in January, April and May, when the cold fronts are strongest (Stallard, 2012a).

Flux chamber measurements found that soils at LEF take up carbonyl sulfide (COS) from the atmosphere (Whelan and Rhew, 2012). Although not directly measured, COS $\delta^{34}S$ value has been estimated to be 11‰ (Newman et al., 1991); however, this COS flux is three orders of magnitude smaller than the sulfate input, and therefore unlikely to significantly affect the isotopic composition of soil S.

5.1.2 S transformations during transport through soil

Rain infiltration rates in the surface soils are greater at Icacos (2-9 cm/min) than at Bisley (0.07-1.5 cm/min), and exceed typical rainfall intensity (0.013 cm/min) at both sites (McDowell et al., 1992). This suggests that, despite the high MAP, soil surfaces rarely become waterlogged. Once in the soil, the rainwater travels downwards mostly via macropores (White et al., 1998), and follows preferred drainage patterns downslope. At Icacos, subsurface water flow is generally deep, below the rooting zone (McDowell et al., 1992), typically along fractures at the saprolite-bedrock interface (White et al., 1998; Kurtz et al., 2011). On the other hand, soil water at Bisley flows within the rooting zone (McDowell et al., 1992). As a result, McDowell et al. (1992)

424 proposed that oxidative processes (degradation of S and nitrification) are segregated in space
425 from reductive processes (plant uptake of S and denitrification) at Icacos, but can coexist at
426 Bisley due to highly variable redox conditions over only fractions of a cm.

427 The depth trends in solid phase S (Figs. 2 and 3) indicate that microbial decomposition may be
428 releasing sulfate depleted in ^{34}S compared to the soil S. For example, in temperate regions the
429 soil solution has lower sulfate $\delta^{34}S$ values than the precipitation (Fuller et al., 1986; Novak et al.,
430 1995; Zhang et al., 1998; Alewell and Gehre, 1999; Alewell et al., 1999). However, we found
431 that during most months, sulfate was enriched by up to 5.6‰ in ^{34}S relative to the solids (Fig. 3).
432 This appears to be due to dissimilatory sulfate reduction in the aqueous phase. Plant uptake also
433 increases pore water $\delta^{34}S$ values, however it is unlikely to affect the deeper samples due to the
434 rooting patterns in these soils. Other mechanisms such as the adsorption/desorption of sulfate
435 (Table A1), produce small isotopic fractionation, and are likely not important here.

436 Our mass balance calculations show that all soils lose pore water sulfate near the surface
437 (between 1.3 and 1.7 g S/(m^2yr)), due to uptake by vegetation, and possibly due to sulfate
438 reduction (thin dashed line in Fig. 5). This sulfate loss is associated with an enrichment in the
439 heavier isotope in pore water by 1.1 to 3.2‰, which is consistent with biological sulfate uptake.
440 The zone of apparent uptake is only 15 cm thick in the lower slope (riparian) soil at Bisley, but is
441 approximately 60 cm thick for all other soils. Below this zone, small losses or gains of sulfate
442 occur with nearly no isotopic fractionation, consistent with oxidative degradation. Our data
443 suggest that the oxidative degradation of organic S, resulting in an influx of sulfate to the pore
444 water with slightly lower $\delta^{34}S$ values, might occur all the way down to the saprolite. The soil-
445 saprolite boundary was identified in the field, based on textural and color changes. For most of
446 these soils, there appears to be a net source of sulfate to pore water in the saprolite region, which

447 could be due to dissolution of sulfide minerals from embedded bedrock corestones. Further work
448 is needed to confirm this. The net result is that as water travels through the soil, it loses sulfate
449 and becomes enriched in the heavy isotopes of S (Fig. 5). The net amount of sulfate lost over the
450 entire soil depth (i.e. losses minus additions occurring above the soil-saprolite boundary) is
451 similar for all soils on quartz diorite and for the volcaniclastic ridgetop soil (between 1.4 and 1.7
452 gS/(m^2yr)). The slope sites on the volcaniclastic parent material lose significantly less sulfate
453 (0.8-0.9 gS/(m^2yr)). The net enrichment in heavier S isotopes is lower on steeper slope sites,
454 potentially as a result of decreased plant uptake due to less dense vegetation on the steeper
455 slopes.

456

457 *5.1.3 Hydrologic S export*

458 Stream sulfate concentrations at baseflow (Table 4) reflect export from soil. McDowell and
459 Asbury (1994) found that N and S concentrations vary minimally with discharge, therefore our
460 baseflow measurements are likely representative of S loss during an entire hydrological year. To
461 estimate the net export of sulfate from the watershed, we multiplied our measured average
462 stream sulfate concentration by the average runoff estimates for the Guaba (3630 mm/yr) and
463 Bisley (2007.5 mm/yr) streams from Stallard and Murphy (2012) and Schellekens et al. (2004)
464 respectively. Our values, 1.7±0.1 g S/(m^2yr) at Icacos, and 2.5±0.2 g S/(m^2yr) at Bisley (Fig. 5),
465 mirror the 2.4 g/(m^2yr) hydrologic export estimated by McDowell and Asbury (1994).

466 At Icacos, stream S export is 0.5 g/(m^2yr) less than the inputs, which means that S accumulates
467 in soil organic matter and/or was released in gaseous form or via sediment losses (Fig. 5). In
468 contrast, the stream S export at Bisley exceeds atmospheric inputs by 0.7 g/(m^2yr), possibly

indicating bedrock sources. Indeed, pyrite and other S-minerals, likely of hydrothermal origin, are present throughout drilled bedrock cores (to 37 m deep) from the Bisley and, to a much lesser extent, in the Icacos watersheds (Buss and White, 2012; Buss et al., 2013). Although this difference between S inputs and exports may be due to the fact that our input values are based on measurements at a higher elevation rather than directly at the sites, the results are consistent with other studies. Stream S export in the Mameyes stream, into which the Bisley stream drains, also exceeds atmospheric inputs (Stallard and Murphy, 2012); rock S may thus be an important component to the hydrologic export at Bisley. At Bisley, N outputs also exceed inputs, suggesting unaccounted-for inputs or a slow depletion of soil organic N (Chestnut et al., 1999).

5.2 Controls on the tropical soil S cycle

Our study design allowed us to investigate how four of the soil forming factors (Jenny, 1941) affect the soil $\delta^{34}S$ values. The impact of time could not be assessed in this study, as both sites are of approximately the same age (soil residence time equals the ratio of soil thickness to denudation rates; Brown et al., 1995).

5.2.1 Climate

The high MAP is a defining characteristic in this ecosystem, affecting the types and rates of processes. Bern et al. (2007) and Bern and Townsend (2008) found that, in similar ecosystems in Costa Rica and Hawaii, dissimilatory sulfate reduction is not a major process despite the high MAP. In the LEF, S isotopes suggest that sulfate reduction occurs, but is spatially and temporally variable.

Given the higher elevation at the Icacos site, rainfall and dust deposition patterns are somewhat different than at Bisley (e.g. Scholl et al., 2009), resulting in a higher sulfate input at Icacos.

492 Icacos receives 700 mm more rainfall per year on average, and derives ~5% of its total
493 precipitation input from cloud water (Pett-Ridge et al., 2009). As a result, we observed higher
494 extractable sulfate concentrations at the soil surface, and greater variability in Cl and sulfate
495 concentrations in pore water. Because Cl and sulfate originate from atmospheric deposition, the
496 differences in their concentrations between the two sites reflect differences in rainfall, dust
497 deposition and/or evapotranspiration rates. The slight differences in MAP also elicit differences
498 in vegetation, which impacts soil C, N and S.
499
500 *5.2.2 Organisms*
501 Although we could not detect a difference between the two sites despite the different vegetation
502 cover types, our isotope data show evidence for extensive biological cycling, including both
503 organic S oxidative degradation and dissimilatory sulfate reduction. The co-occurrence of these
504 two processes in LEF soils is supported by similar results for N (Pett-Ridge et al., 2006) and by
505 other studies showing the co-occurrence of saturated and unsaturated processes due to spatial
506 segregation in these soils (McSwiney et al., 2001).
507 Compared to the soil, vegetation litter is approximately 1‰ depleted in ^{34}S (Fig. 7). Differences
508 between soil and vegetation $\delta^{34}S$ were also observed in Costa Rica (Bern et al., 2007), and have
509 been reported for some temperate sites as well. Such a small difference between the $\delta^{34}S$ of total
510 S in soils and vegetation litter might be regarded as evidence for little to no isotopic fractionation
511 during plant uptake and assimilation. However, since plants take up S mostly as sulfate, litter
512 $\delta^{34}S$ must be compared with rain and pore water $\delta^{34}S$ to evaluate this issue. Our data show that
513 the fresh litter is 3 to 5‰ depleted in ^{34}S compared to the average pore water (Fig. 3). This
514 suggests that plants discriminate against the heavier isotope in the process of sulfate uptake and

assimilation. A distinctive, albeit relatively small, fractionation during S assimilation is common also for other life forms. For instance, S metabolism studies with bacteria, algae and yeast (Table A1) found that assimilated S can be up to 2.8‰ depleted compared to its source (Kaplan and Rittenberg, 1964). Another potential source of fractionation occurred during S retranslocation and the beginning of decomposition of the fresh leaves. Plants also fractionate S isotopes via H_2S emissions when stressed by high S inputs, (Trust and Fry, 1992), but given the low S loading at our sites, we suspect plant H_2S emissions by plants are insignificant.

5.2.3 Topography

Our sites were chosen to capture the topographic variation in weathering and pore waters from ridge to valley. Topography is known to impact N cycling in different climates (e.g. Robertson et al., 1988; Raghubanshi, 1992; Roy and Singh, 1994; Chestnut et al., 1999). In the LEF, previous studies have shown that changing redox conditions with topographic location affect N_2O production (McSwiney et al., 2001). We found that the C, N and S content (mg/kg soil) of the mineral soil in the upper meter decrease downslope at all sites, while soil surface $\delta^{15}N$ values decrease downslope at the Bisley site only. The lower slope site at Bisley has the lowest C, N and S content, and the highest $\delta^{15}N$ and lowest $\delta^{34}S$ values, indicating that reduction processes are important. Soils at this site are wetter and more gray in color than those at the other sites, where $\delta^{34}S$ values seem unaffected by topography.

5.2.4 Lithology

Soil and pore water $\delta^{34}S$ values (e.g. Fig. 3) are closer to input chemistry (Table 2) than to typical values for reduced S minerals in rocks (Table A2), reflecting little to no contribution of bedrock S to soils. Compared to the volcaniclastic bedrock, the quartz diorite contains few S minerals and only in a few discrete zones (e.g., Buss et al., 2008; 2013; Buss and White, 2012), but we found no significant difference in $\delta^{34}S$ values in the deep soils at the two sites that could indicate a lithologic impact. In contrast, once the water leaves the weathered soil and enters saprolite, lithologic inputs are significant at Bisley (below 180 cm) and in the stream at baseflow, given the very low $\delta^{34}S$ value (1.6±0.7‰). It then appears that bedrock S is lost to the groundwater before the saprolite converts to soil. Indeed, the 37+ m of saprolite in Bisley contains abundant, highly fractured bedrock corestones containing sulfide minerals (Buss et al., 2013). In contrast, the Icacos baseflow $\delta^{34}S$ value (19.5±1.6‰) is similar to that of atmospheric inputs, signifying minimal lithologic input of S.

5.3 Comparison of the S and N cycles in tropical soils

To understand the degree of coupling or similarity between the S and N cycles, we studied the isotope effects during transport through soil of the dissolved and solid organic matter. Advection is likely the main transport process here, because inputs occur mainly at or near the surface: roots and earthworms diffusively mix the upper 16-17 cm (Table 1), and plant litter is added to the O horizons. An advection model supports that a linear relationship should exist between soil δ values and $\ln f$ (Eqn. 10). We found a linear relationship between $\delta^{15}N$ and $\ln(N\%)$, but not between $\delta^{34}S$ and $\ln(S\%)$ (Fig. 6). There are therefore some key differences between N and S biogeochemistry in these soils. The advection model assumes constant v, k and α with depth

(Baisden et al., 2003), so one or more of these parameters must vary for S. Since ν and k are parameters that should be similar for N and S, the S isotope fractionation factor α is most likely the reason for the contrast between N and S.

We calculated the fractionation factors for the soils examined through trenching. For N, the depth-insensitive fractionation factors (Eqn. 11) are all smaller than 1, showing enrichment in the heavier isotope due to oxidative degradation of the organic matter (in the topmost (A) horizon) as it is moved downward in the soil profile. For S, since α changes with depth, we computed the fractionation factor α between soil layers by applying Eqn. 11 to each layer using the layer above as the S input. The results show large variations in α with depth (Fig. A2 in the Appendix), with both: (1) α values less than 1, indicative of oxidative degradation, or successive cycles of oxidative degradation and assimilation, and (2) α values greater than 1, indicative of dissimilatory sulfate reduction, which leads to depleted reduced S compounds that are removed, thus enriching the soil in ^{34}S.

Thus, these results suggest a decoupling of, or differences in, the soil N and S cycles, particularly in terms of redox reactions. Denitrification should be thermodynamically favored over dissimilatory sulfate reduction, since it has a higher Gibbs free energy yield (Zehnder and Stumm, 1988). Thus, the greater apparent redox sensitivity of S compared to N is unexpected. The most likely explanation is that the isotope fractionation effects associated with S reduction are enhanced compared to those of denitrification due to the greater relative biological demand for N than for S. S is in greater biological excess than N in these soils, as evidenced by the generally low N:S ratios (Fig. 4). If N becomes limiting, the observable fractionation will be greatly reduced due to near complete consumption of the nitrate by any biological fractionating process, unless reduced N trace gasses leave the system. Because S is likely in low biological

demand, it is less likely to be completely consumed by any process, and therefore the observed isotope effects will be greater. Furthermore, sulfate adsorbs on iron and aluminum oxides and, instead of being lost in gaseous form, reduced S species are generally reoxidized and/or assimilated into organic matter (Alewell and Novak, 2001), which can subsequently re-experience oxidative degradation and reduction. In contrast, nitrate is poorly absorbed in soils, and reduced N species easily leave the soil in gaseous forms. In general, it appears that S isotopes reflect an integrative view of multiple cycles of reduction and oxidation processes.

6. CONCLUSIONS AND OUTLOOK

This study of S biogeochemistry in two Puerto Rican watersheds (Icacos and Bisley) combined a comparative analysis of stable N and S isotope measurements in the soil with S isotope measurements in atmospheric inputs, pore water, stream water at baseflow and groundwater. In most ecosystems, the LEF included, S cycling depends entirely on the steady supply of sulfate from a variety of atmospheric sources. This Puerto Rican rainforest currently receives a portion of its S from anthropogenic sources in North America and the eastern side of the Atlantic. We found that stream S export is 0.5 g/(m^2yr) less than the inputs at Icacos, but 0.7 g/(m^2yr) more at Bisley. This suggests that there may be yet-unaccounted loss pathways at Icacos (e.g. gaseous emissions or sediment transport), and input pathways at Bisley (e.g. lithogenic). The volcaniclastic rock likely delivers S to the stream, but not to the soil, and therefore the soil-plant system depends on atmospheric inputs. We found no indication that parent material impacts S biogeochemistry within the soils. Topography, on the other hand, affects the S cycle through redox conditions. Climate is the main abiotic factor driving S cycling in the LEF, especially the high MAP, which determines the types and rates of processes. Biological cycling is extensive,

and our data support the co-occurrence of three major S-fractionating processes in these soils: plant uptake, oxidative degradation of organic S and dissimilatory bacterial sulfate reduction. The rate and importance of these processes vary in time and space, and their co-occurrence dampens their individual signals. An advection/decomposition model agreed well with the N data, however the assumption of a constant fractionation factor α with depth failed for S. This is a fundamental difference between N and S cycling in these soils, likely because S is in less biological demand and more likely recycled than lost in gaseous forms compared to N.

The ecosystem's dependence on atmospheric S inputs implies that any changes in the amount of rain or the amount of sulfate in rain will drive the system out of its present steady state. In the LEF, climate change and deforestation may decrease orographic rains, which are responsible for 29-35% of the precipitation in this rainforest (Scholl et al., 2009). Such decreases in MAP could begin to deplete the soil organic S (and N) pool. In addition to changing rain patterns, deforestation also has a more direct effect on S cycling since vegetation assimilates and retains atmospheric sulfate in the soil. Disturbances in vegetation cover may thus accelerate S losses and decrease the soil organic S pool.

ACKNOWLEDGEMENTS

Logistical support and data were provided by the NSF-supported Luquillo Critical Zone Observatory (EAR-0722476) with additional support provided by the USGS Luquillo WEBB program and the USDA Forest Service International Institute of Tropical Forestry. We thank the USGS for installing LGW1, K. Finstad, S. Hall, M. Whelan and M. Rosario for technical assistance in the field, and M. C. Torrens, S. Moya, J. Carlos and J. Orlando for sample

collection. We are also grateful to the late F. Scatena for his invaluable logistical support, to M. Leon for providing maps of the study area, to A. Kirk and A. Engelbrektson for laboratory assistance, and to J. Coates, W. Yang, P. Brooks and S. Mambelli for access to instruments and sample analysis.

REFERENCES

Acquaye D. K. and Beringer H. (1989) Sulfur in Ghanaian Soils .1. Status and Distribution of Different Forms of Sulfur in some Typical Profiles. *Plant Soil* **113,** 197-203.

Alewell C. and Gehre M. (1999) Patterns of stable S isotopes in a forested catchment as indicators for biological S turnover. *Biogeochemistry* **47,** 319-333.

Alewell C. and Novak M. (2001) Spotting zones of dissimilatory sulfate reduction in a forested catchment: the S-34-S-35 approach. *Environ. Pollut.* **112,** 369-377.

Alewell C., Mitchell M. J., Likens G. E. and Krouse H. R. (1999) Sources of stream sulfate at the Hubbard Brook Experimental Forest: Long-term analyses using stable isotopes. *Biogeochemistry* **44,** 281-299.

Amundson R., Austin A. T., Schuur E. A. G., Yoo K., Matzek V., Kendall C., Uebersax A., Brenner D. and Baisden W. T. (2003) Global patterns of the isotopic composition of soil and plant nitrogen. *Global Biogeochem. Cycles* **17***(1)***,** 1031, doi:10.1029/2002GB001903.

Amundson R., Barnes J. D., Ewing S., Heimsath A. and Chong G. (2012) The stable isotope composition of halite and sulfate of hyperarid soils and its relation to aqueous transport. *Geochim. Cosmochim. Acta* **99,** 271-286.

646 Asbury C. E., Mcdowell W. H., Trinidadpizarro R. and Berrios S. (1994) Solute Deposition from
647 Cloud-Water to the Canopy of a Puerto-Rican Montane Forest. *Atmos. Environ.* **28,** 1773-
648 1780.

649 Austin A. T. and Vitousek P. M. (1998) Nutrient dynamics on a precipitation gradient in Hawai'i.
650 *Oecologia* **113,** 519-529.

651 Bern C. R., Porder S. and Townsend A. R. (2007) Erosion and landscape development decouple
652 strontium and sulfur in the transition to dominance by atmospheric inputs. *Geoderma* **142,**
653 274-284.

654 Bern C. R. and Townsend A. R. (2008) Accumulation of atmospheric sulfur in some Costa Rican
655 soils. *J Geophys Res-Biogeo* **113,** G03001.

656 Bhatt M. P. and McDowell W. H. (2007) Controls on major solutes within the drainage network
657 of a rapidly weathering tropical watershed. *Water Resour. Res.* **43,** W11402.

658 Boccheciamp R. A. (1977) Soil survey of the Humacao area of eastern Puerto Rico. *USDA Soil*
659 *Conserv. Serv.*

660 Bradley A. S., Leavitt W. D. and Johnston D. T. (2011) Revisiting the dissimilatory sulfate
661 reduction pathway. *Geobiology* **9,** 446-457.

662 Brandmeier M., Kuhlemann J., Krumrei I., Kappler A. and Kubik P. W. (2011) New challenges
663 for tafoni research. A new approach to understand processes and weathering rates. *Earth*
664 *Surf. Process. Landforms* **36,** 839-852.

665 Brenner D. L. (1999). Soil nitrogen isotopes along natural gradients: models and measurements.
666 M.S. thesis, University of California, Berkeley, CA.

667 Brown E. T., Stallard R. F., Larsen M. C., Raisbeck G. M. and Yiou F. (1995) Denudation rates
668 determined from the accumulation of in situ produced ^{10}Be in the Luquillor Experimental
669 Forest, Puerto Rico. *Earth Plant. Sci. Lett.* **129,** 139-202.

670 Bruchert V., Knoblauch C. and Jorgensen B. B. (2001) Controls on stable sulfur isotope
671 fractionation during bacterial sulfate reduction in Arctic sediments. *Geochim. Cosmochim.*
672 *Acta* **65,** 763-776.

673 Brunner B. and Bernasconi S. M. (2005) A revised isotope fractionation model for dissimilatory
674 sulfate reduction in sulfate reducing bacteria. *Geochim. Cosmochim. Acta* **69,** 4759-4771.

675 Buss H. L., Sak P. B., Webb S. M. and Brantley, S. L. (2008) Weathering of the Rio Blanco
676 quartz diorite, Luquillo Mountains, Puerto Rico: Coupling oxidation, dissolution, and
677 fracturing. *Geochim. Cosmochim. Acta* **72,** 4488-4507

678 Buss H. L., Mathur R., White A. F. and Brantley S. L. (2010) Phosphorus and iron cycling in
679 deep saprolite, Luquillo Mountains, Puerto Rico. *Chem. Geol.* **269,** 52-61.

680 Buss H. L., White A. F., Blum A. E., Schulz M. S. and Vivit D. (2011) Long-term versus short-
681 term weathering fluxes in contrasting lithologies at the Luquillo Critical Zone Observatory,
682 Puerto Rico. *Mineral Mag* **75**(3), p. 604.

683 Buss H. L. and White A. F. (2012) Weathering Processes in the Rio Icacos Watershed. In:
684 Murphy S.F. and Stallard R.F., eds, *Water Quality and Landscape Processes of Four*
685 *Watersheds in Eastern Puerto Rico:* U.S. Geological Survey Professional Paper 1789, pp.
686 249-262. http://pubs.usgs.gov/pp/1789/.

687 Buss H. L., Brantley S. L., Scatena F. N., Bazilievskaya E. A., Blum A., Schulz M., Jimenez R.,
688 White A. F., Rother G., Cole D. (2013) Probing the deep critical zone beneath the Luquillo
689 Experimental Forest, Puerto Rico. *Earth Surf. Proc. Land.* **38**, 1170-1186. DOI:
690 10.1002/esp.3409

691 Calhoun J. A., Bates T. S. and Charlson R. J. (1991) Sulfur Isotope Measurements of
692 Submicrometer Sulfate Aerosol-Particles Over the Pacific-Ocean. *Geophys. Res. Lett.* **18,**
693 1877-1880.

694 Canfield D. E., Olesen C. A. and Cox R. P. (2006) Temperature and its control of isotope
695 fractionation by a sulfate-reducing bacterium. *Geochim. Cosmochim. Acta* **70,** 548-561.

696 Chestnut T. J., Zarin D. J., McDowell W. H., Keller M. (1999) A nitrogen budget for late-
697 successional hillslope tabonuco forest, Puerto Rico, *Biogeochemistry*, **46**, 85-108.

698 Chukrov F. V., Ermilova L. P., Chukirov V. S. and Nosik L. P. (1980) The isotopic composition
699 of plant sulfur. *Org. Geochem.* **2**, 69 – 75.

700 Cox S. B., Willig M. R. and Scatena F. N. (2002) Variation in nutrient characteristics of surface
701 soils from the Luquillo Experimental Forest of Puerto Rico: A multivariate perspective.
702 *Plant Soil* **247,** 189-198.

703 Delmas R., Baudet J. and Servant J. (1978) Natural sources of sulfate in humid tropical
704 environment. *Tellus* **30,** 158-168.

705 Delmas R. and Servant J. (1983) Atmospheric balance of sulfur above an equatorial forest. *Tellus*
706 *B* **35,** 110-120.

Ewing S. A., Yang W., DePaolo D. J., Michalski G., Kendall C., Stewart B. W., Thiemens M. and Amundson R. (2008) Non-biological fractionation of stable Ca isotopes in soils of the Atacama Desert, Chile. *Geochim. Cosmochim. Acta* **72,** 1096-1110.

Fry B., Gest H. and Hayes J. M. (1988a) S-34/s-32 Fractionation in Sulfur Cycles Catalyzed by Anaerobic-Bacteria. *Appl. Environ. Microbiol.* **54,** 250-256.

Fry B., Ruf W., Gest H. and Hayes J. M. (1988b) Sulfur Isotope Effects Associated with Oxidation of Sulfide by O-2 in Aqueous-Solution. *Chem. Geol.* **73,** 205-210.

Fuller R. D., Mitchell M. J., Krouse H. R., Wyskowski B. J. and Driscoll C. T. (1986) Stable Sulfur Isotope Ratios as a Tool for Interpreting Ecosystem Sulfur Dynamics. *Water Air Soil Poll* **28,** 163-171.

Garcia-Martino A. R., Warner G. S., Scatena F. N. and Civco D. L. (1996) Rainfall, runoff and elevation relationships in the Luquillo Mountains of Puerto Rico. *Caribb J Sci* **32,** 413-424.

Gould W. A., Gonzalez G. and Carrero Rivera G. (2006) Structure and composition of vegetation along an elevational gradient in Puerto Rico. *J. Veg. Sci.* **17,** 563-574.

Gravenhorst G. (1978) Maritime Sulfate Over North-Atlantic. *Atmos. Environ.* **12,** 707-713.

Harris E., Sinha B., Foley S., Crowley J. N., Borrmann S. and Hoppe P. (2012) Sulfur isotope fractionation during heterogeneous oxidation of SO2 on mineral dust. *Atmos Chem Phys* **12,** 4867-4884.

Heartsill-Scalley T., Scatena F. N., Estrada C., McDowell W. H. and Lugo A. E. (2007) Disturbance and long-term patterns of rainfall and throughfall nutrient fluxes in a subtropical wet forest in Puerto Rico. *J Hydrol* **333,** 472-485.

728 Huffaker L. (2002) Soil Survey of Caribbean National Forest and Luquillo Experimental Forest,
729 Commonwealth of Puerto Rico. USDA, NRCS, Washington, DC.

730 Johnston M. H. (1992) Soil-Vegetation Relationships in a Tabonuco Forest Community in the
731 Luquillo Mountains of Puerto-Rico. *J. Trop. Ecol.* **8,** 253-263.

732 Kaplan I. R. and Rafter T. A. (1958) Fractionation of Stable Isotopes of Sulfur by Thiobacilli.
733 *Science* **127,** 517.

734 Kaplan I. R. and Rittenberg S. C. (1964) Microbiological Fractionation of Sulphur Isotopes. *J.*
735 *Gen. Microbiol.* **34,** 195-212.

736 Keene W. C., Pszenny A. A. P., Galloway J. N. and Hawley M. E. (1986) Sea-Salt Corrections
737 and Interpretation of Constituent Ratios in Marine Precipitation. *J Geophys Res-Atmos* **91,**
738 6647-6658.

739 Kurtz A.C., Lugolobi F., Salvucci G. (2011) Germanium-silicon as a flow path tracer:
740 Application to the Rio Icacos watershed. *Water Resour. Res.* **47**, W06516.
741 DOI: 10.1029/2010WR009853.

742 Likens G. E., Driscoll C. T., Buso D. C., Mitchell M. J., Lovett G. M., Bailey S. W., Siccama T.
743 G., Reiners W. A. and Alewell C. (2002) The biogeochemistry of sulfur at Hubbard Brook.
744 *Biogeochemistry* **60,** 235-316.

745 Marty C., Houle D., Gagnon C. and Duchesne L. (2011) Isotopic compositions of S, N and C in
746 soils and vegetation of three forest types in Quebec, Canada. *Appl. Geochem.* **26,** 2181-
747 2190.

McDowell W. H. and Asbury C. E. (1994) Export of Carbon, Nitrogen, and Major Ions from 3 Tropical Montane Watersheds. *Limnol. Oceanogr.* **39,** 111-125.

McDowell W. H., Sanchez C. G., Asbury C. E. and Perez C. R. R. (1990) Influence of Sea Salt Aerosols and Long-Range Transport on Precipitation Chemistry at El-Verde, Puerto-Rico. *Atmos Environ A-Gen* **24,** 2813-2821.

McDowell W. H., Bowden W. B. and Asbury C. E. (1992) Nitrogen dynamics in two geomorphologically distinct tropical rain forest watersheds: subsurface solute patterns. *Biogeochemistry* **18,** 53-75.

McSwiney C. P., McDowell W. H. and Keller M. (2001) Distribution of nitrous oxide and regulators of its production across a tropical rainforest catena in the Luquillo Experimental Forest, Puerto Rico. *Biogeochemistry* **56***(3)*, 265-286.

Murphy S. F., Brantley S. L., Blum A. E., White A. F. and Dong H. (1998) Chemical weathering in a tropical watershed, Luquillo Mountains, Puerto Rico: II Rate and mechanisms of biotite weathering. *Geochim. Cosmochim. Acta.* **62***(2)*, 227-243.

Murphy S. F. and Stallard R. F. (2012) Hydrology and climate of four watersheds in Eastern Puerto Rico. In *Water quality and landscape processes of four watersheds in Eastern Puerto Rico*: U.S. Geological Survey Professional Paper 1789 (eds. S. F. Murphy and R. F. Stallard). USGS, Reston, VA. 292 p.

Murphy S. F., Stallard R. F., Larsen M. C. and Gould W. A. (2012) Physiography, geology and land cover of four watersheds in Eastern Puerto Rico. In *Water quality and landscape*

processes of four watersheds in Eastern Puerto Rico: U.S. Geological Survey Professional Paper 1789 (eds. S. F. Murphy and R. F. Stallard). USGS, Reston, VA. 292 p.

Newman L., Krouse H. R. and Grinenko V. A. (1991) Sulphur isotope variations in the atmosphere. In *Stable Isotopes in the Assessment of Natural and Anthropogenic Sulphur in the Environment* (eds. H. R. Krouse and V. A. Grinenko). SCOPE, vol. 43. John Wiley and Sons Ltd, Chichester. pp. 133-176.

Nielsen H., Pilot J., Grinenko L. N., Grinenko V. A., Lein A. Y., Smith J. W. and Paninka R. G. (1991) Lithospheric sources of sulfur. In *Stable Isotopes in the Assessment of Natural and Anthropogenic Sulphur in the Environment.* SCOPE, vol. 43. (eds. H. R. Krouse and V. A. Grinenko). John Wiley and Sons Ltd, Chichester. pp. 65-132.

Norman A. L. (1994) Isotope analysis of microgram quantities of sulfur: Applications to soil sulfur mineralization studies. PhD thesis, Univ. of Calgary, Canada.

Norman A. L., Giesemann A., Krouse H. R. and Jager H. J. (2002) Sulphur isotope fractionation during sulphur mineralization: Results of an incubation-extraction experiment with a Black Forest soil. *Soil Biol. Biochem.* **34,** 1425-1438.

Novak M., Bottrell S. H., Groscheova H., Buzek F. and Cerny J. (1995) Sulphur isotope characteristics of two North Bohemian forest catchments. *Water Air Soil Poll* **85,** 1641-1646.

Novak M., Bottrell S. H. and Prechova E. (2001) Sulfur isotope inventories of atmospheric deposition, spruce forest floor and living Sphagnum along a NW-SE transect across Europe. *Biogeochemistry* **53,** 23-50.

789 Pett-Ridge J., Silver W. L. and Firestone M. K. (2006) Redox fluctuations frame microbial
790 community impacts on N-cycling rates in a humid tropical forest soil. *Biogeochemistry* **81,**
791 95-110.

792 Pett-Ridge J. C. (2009) Contributions of dust to phosphorus cycling in tropical forests of the
793 Luquillo Mountains, Puerto Rico. *Biogeochemistry* **94,** 63-80.

794 Pett-Ridge J. C., Derry L. A. and Kurtz A. C. (2009) Sr isotopes as a tracer of weathering
795 processes and dust inputs in a tropical granitoid watershed, Luquillo Mountains, Puerto
796 Rico. *Geochim. Cosmochim. Acta* **73,** 25-43.

797 Poulson S. R., Kubilius W. P. and Ohmoto H. (1991) Geochemical Behavior of Sulfur in
798 Granitoids during Intrusion of the South Mountain Batholith, Nova-Scotia, Canada.
799 *Geochim. Cosmochim. Acta* **55,** 3809-3830.

800 Prietzel J. and Mayer B. (2005) Isotopic fractionation of sulfur during fonnation of basaluminite,
801 alunite, and natroalunite. *Chem. Geol.* **215,** 525-535.

802 Rees C. E., Jenkins W. J. and Monster J. (1978) Sulfur Isotopic Composition of Ocean Water
803 Sulfate. *Geochim. Cosmochim. Acta* **42,** 377-381.

804 Sakai H., Casadevall T. J. and Moore J. G. (1982) Chemistry and Isotope Ratios of Sulfur in
805 Basalts and Volcanic Gases at Kilauea Volcano, Hawaii. *Geochim. Cosmochim. Acta* **46,**
806 729-738.

807 Sakai H., Desmarais D. J., Ueda A. and Moore J. G. (1984) Concentrations and Isotope Ratios of
808 Carbon, Nitrogen and Sulfur in Ocean-Floor Basalts. *Geochim. Cosmochim. Acta* **48,** 2433-
809 2441.

Savoie D. L., Prospero J. M. and Saltzman E. S. (1989) Non-Sea-Salt Sulfate and Nitrate in Trade-Wind Aerosols at Barbados - Evidence for Long-Range Transport. *J Geophys Res-Atm* **94,** 5069-5080.

Scatena F. N. (1989) An introduction to the physiography and history of the Bisley Experimental Watersheds in the Luquillo Mountains of Puerto Rico. *General Technical Report - Southern Forest Experiment Station, USDA Forest Service*

Schellekens J., Scatena F. N., Bruijnzeel L. A., van Dijk A. I. J. M, Groen M. M. A. and Hogezand R. J. P. (2004) Stormflow generation in a small rainforest catchment in the Luquillo Experimental Forest, Puerto Rico. *Hydrol. Process.* **18,** 505-530.

Schoeneberger P. J., Wysocki D. A., Benham E. C., and Broderson W. D. (eds.) (2002) Field book for describing and sampling soils, Version 2.0. NRCS, National Soil Survey Center, Lincoln, NE.

Scholl M. A., Shanley J. B., Zegarra J. P. and Coplen T. B. (2009) The stable isotope amount effect: New insights from NEXRAD echo tops, Luquillo Mountains, Puerto Rico. *Water Resour. Res.* **45,** W12407.

Silver W. L., Scatena F. N., Johnson A. H., Siccama T. G. and Sanchez M. J. (1994) Nutrient Availability in a Montane Wet Tropical Forest - Spatial Patterns and Methodological Considerations. *Plant Soil* **164,** 129-145.

Sim M. S., Bosak T. and Ono S. (2011) Large Sulfur Isotope Fractionation Does Not Require Disproportionation. *Science* **333,** 74-77.

Soil Survey Staff, Natural Resources Conservation Service, United States Department of Agriculture. Web Soil Survey. Available online at http://websoilsurvey.nrcs.usda.gov/. Accessed [05/15/2013].

Stallard R. F. (2012a) Atmospheric inputs to watersheds of the Luquillo Mountains in Eastern Puerto Rico. In *Water quality and landscape processes of four watershed in eastern Puerto Rico*: U.S. Geological Survey Professional Paper 1789 (eds. S. F. Murphy and R. F. Stallard). USGS, Reston, VA. 292 p.

Stallard R. F. (2012b) Weathering, landscape equilibrium, and carbon in four watersheds in eastern Puerto Rico. In *Water quality and landscape processes of four watershed in eastern Puerto Rico*: U.S. Geological Survey Professional Paper 1789 (eds. S. F. Murphy and R. F. Stallard). USGS, Reston, VA. 292 p.

Stallard R. F. and Murphy S. F. (2012) Water quality and mass transport in four watersheds in Eastern Puerto Rico. In *Water quality and landscape processes of four watersheds in Eastern Puerto Rico*: U.S. Geological Survey Professional Paper 1789 (eds. S. F. Murphy and R. F. Stallard). USGS, Reston, VA. 292 p.

Stanko-Golden K. M. and Fitzgerald J. W. (1991) Sulfur Transformations and Pool Sizes in Tropical Forest Soils. *Soil Biol. Biochem* **23,** 1053-1058.

Stempvoort D. R. v., Reardon E. J. and Fritz P. (1990) Fractionation of sulfur and oxygen isotopes in sulfate by soil sorption. *Geochim. Cosmochim. Acta* **54,** 2817-2826.

Tabatabai M. A. (1984) Importance of Sulfur in Crop Production. *Biogeochemistry* **1,** 45-62.

Thode H. G. and Monster J. (1965) Sulfur-isotope geochemistry of petroleum, evaporates, and ancient seas. In *Fluids in Subsurface Environments* (eds. Young A. and J. E. Galley), *Mem. Am. Assoc. Petrol. Geol.* **4,** 367–377.

Trust B. A. and Fry B. (1992) Stable Sulfur Isotopes in Plants - a Review. *Plant Cell Environ* **15,** 1105-1110.

Turchyn A. V., Bruchert V., Lyons T. W., Engel G. S., Balci N., Schrag D. P. and Brunner B. (2010) Kinetic oxygen isotope effects during dissimilatory sulfate reduction: A combined theoretical and experimental approach. *Geochim. Cosmochim. Acta* **74,** 2011-2024.

Vitousek P. M. and Sanford R. L. (1986) Nutrient Cycling in Moist Tropical Forest. *Annu. Rev. Ecol. Syst.* **17,** 137-167.

Weaver P. L. and Murphy P. G. (1990) Forest structure and productivity in Puerto Rico's Luquillo Mountains. *Biotropica* **22**(1), 69-82.

Whelan M. and Rhew R. (2012) Effects of rainfall on terrestrial fluxes of global cooling gases: carbonyl sulfide (COS) and its precursor dimethyl sulfide (DMS). Abstract B44C-07, presented at 2012 Fall Meeting, AGU, San Francisco, Calif., 3-7 Dec.

White A. F., Blum A. E., Schulz M. S., Vivit D. V., Stonestrom D. A., Larsen M., Murphy S. F. and Eberl D. (1998) Chemical weathering in a tropical watershed, Luquillo mountains, Puerto Rico: I. Long-term versus short-term weathering fluxes. *Geochim. Cosmochim. Acta* **62,** 209-226.

White A. F., Schulz M. S., Stonestrom D. A., Vivit D. V., Fitzpatrick J., Bullen T. D., Maher K. and Blum A. E. (2009) Chemical weathering of a marine terrace chronosequence, Santa

Cruz, California. Part II: Solute profiles, gradients and the comparisons of contemporary and long-term weathering rates. *Geochim. Cosmochim. Acta* **73,** 2769-2803.

Zehnder A. J. B. and Stumm W. (1988) Geochemistry and biogeochemistry of anaerobic habitats. In *Biology of Anaerobic Microorganisms* (ed. A. J. N. Zehnder). Wiley, New York, pp 469-585.

Zhang Y. M., Mitchell M. J., Christ M., Likens G. E. and Krouse H. R. (1998) Stable sulfur isotopic biogeochemistry of the Hubbard Brook Experimental Forest, New Hampshire. *Biogeochemistry* **41,** 259-275.

Zou X. M., Zucca C. P., Waide R. B. and McDowell W. H. (1995) Long-term influence of deforestation on tree species composition and litter dynamics of a tropical rain-forest in Puerto-Rico. *Forest Ecol. Manag.* **78**(1-3), p. 147-157.

1 **TABLES**

2 Table 1: Field data for the Icacos and Bisley soils from pits dug at the highest topographic location (ridge
3 shoulder and ridgetop respectively). Nomenclature according to NRCS guidelines (Schoeneberger et al.,
4 2002).

Horizon	Top [cm]	Bottom [cm]	Color	Texture	Clay %	Structure	Roots	Features
Icacos								
O	3	0						
A1	0	7.5	10YR 4/6	cl	34	3 f,c sbk	2vf, 2f, 1m, 1c	
A2	7.5	16	10YR 5/6	cosc	37	2 f,c sbk	1vf, 1f, 1c	
Btg1	16	30	10YR 7/2, 7/6; 7.5YR 6/8	cosc	40	3 c,vc sbk	1vf	
Btg2	30	45	10YR 7/2, 7/6; 7.5YR 5/8; 5YR 5/8	sc	>40	2 m,c sbk	1vf	
Btv	45	75	5YR 5/8; 10YR 6/8; 10YR 4/4	c (or vfsc)	>40	2 c,vc sbk	1vf	plinthite; dark spots with humus and Mn
Bt1	75	85	10YR 2/1; 7.5YR 6/4; 5YR 4/4; 2.5YR 4/6	cosc	35	2 m,c sbk	0	Mn-rich zone
Bt2	85	102	2.5YR 4/6	cl	38	2 m,c sbk	0	white quartz and mica-rich; smooth
Btg3	102	111	5YR 8/1; 5YR 6/6	c	>40	2 m sbk	0	
Crt	111	127	2.5YR 3/4, 5YR 5/8, 7.5YR 7/5	grls	3	rock texture	0	oxidized saprolite with black Mn oxides
Bisley								
O	2	0	10YR 5/6				mat below litter	highly mixed
A1	0	10	10YR 5/6	cl	38-40	3 f,m sbk	3vf, 3f, 2m, 2c	highly mixed
A2	10	17	10YR 6/8, 5/6	c	45	3 f sbk	2vf, 2f, 1m, 1c	
Btg1	17	40	10YR 7/8; 7.5YR 6/8	c	>45	2 c abk	1vf, 1f, 1c	
Bt1	40	66	5YR 6/8; 10YR 5/6	c	>45	2 c abk → 2 f abk	1vf, 1f	
Bt2	66	95	2.5YR 6/8, 6/6; 10YR 7/8	c	>45	2 c sbk → 2 m sbk	1vf, 1f	white saprolite flakes mixed in; some reduced spots
Bt3	95	102	10R 5/6; 7.5YR 5/6	c	>45	2 m,c sbk	1vf	flakes of saprolite
Btg2	102	142	5YR 5/6; 10R 5/6; 7.5YR 6/8	c	40-45	2 m,c sbk	1vf	
Crt	142	158	10R 5/8	cl	36	2 c sbk	1vf	many white flakes of kaolinized grus

Table 2: The C, N and S composition of vegetation and O horizon (litter layer) at the Icacos and Bisley sites. Analytical error is 0.1‰ for C and N isotopes and 5% of the value for C and N concentration; analytical error for S it is 0.6‰ for isotopes and 350 mg/kg for concentration.

Sample type*	C %	$\delta^{13}C$ [‰]	N %	$\delta^{15}N$ [‰]	S [mg/kg]	$\delta^{34}S$ [‰]	C:N	C:S	N:S
Icacos:									
ground ferns	39.40	-32.9	1.37	-0.41	2266	13.9	29	174	6:1
Bromeliads (family Bromeliaceae)	45.63	-29.9	0.62	-2.5	1076	13.8	74	424	6:1
Heliconia (family Heliconiaceae)	48.01	-28.5	1.08	1.0	1018	13.2	45	471	11:1
ferns	44.90	-32.3	1.51	1.8	2078	13.8	30	216	7:1
Sierra Palm (*Prestoea Montana*)	45.18	-30.2	1.49	-2.9	7150	15.5	30	63	2:1
Colorado (*Cyrilla racemiflora*)	51.51	-33.2	0.95	0.97	1671	15.4	54	308	6:1
O horizon (3-0 cm)	50.41	-29.7	0.64	-0.63	965	12.9	78	522	7:1
Bisley:									
Tabonuco (*Dacryodes excelsa*)	45.38	-36.0	1.67	-0.51	1791	14.9	27	253	9:1
Sierra Palm (*Prestoea Montana*)	43.44	-31.7	1.41	-1.7	4354	16.0	31	100	3:1
O horizon (2-0 cm)	32.97	-30.0	1.13	-0.04	1040	13.3	29	317	11:1

* All samples are whole leaves or leaf fragments collected from the forest floor in May 2010. Samples were run at least in duplicates, with very good precision and quality control.

Table 3: Anion chemistry of the East Peak precipitation samples. Missing isotope values indicate samples that had insufficient S due to low sulfate concentration and/or low sample volume.

Sampling date	Cl [μM]	SO_4 [μM]	SO_4 $\delta^{34}S$ [‰]	% nss-SO_4**	Calculated nss-SO_4 $\delta^{34}S$ [‰]***
6/1/10	18	7.3		87	
7/6/10	46	11.1	12.6	78	10.3
8/3/10	164	19.4	18.3	56	16.1
9/7/10*	76	10.9	17.9	64	16.1
10/5/10*	35	12.4	15.8	85	14.9
11/2/10	110	13.6	16.6	58	13.5
12/14/10*	37	9.5		80	
1/25/11	118	26.2		77	
2/8/11	158	12.8		36	
3/8/11	148	10.4	18.5	26	11.1
4/5/11	226	38.8	10.7	70	6.3
5/17/11	18	5.4		83	
6/7/11	19	8.2	12.3	88	11.0
7/19/11	196	23.1	17.6	56	14.9
8/9/11	56	10.8	17.2	73	15.7
9/6/11	27	4.6	18.0	69	16.7
10/11/11	61	13.4		76	
11/8/11*	38	13.2	20.5	85	20.5

1/3/12	113	13.9	14.7	58	10.1
1/31/12	164	12.7	21.4	33	22.3
3/13/12*	125	14.4	15.8	55	11.6
6/26/12	166	24.5	16.0	65	13.2
average (volume-weighed)	***116 ± 65***	***15.9 ± 7.9***	***16.1 ± 2.8***	***63 ± 18***	***13.4 ± 4.0***

* These samples were not included in the volume-weighted averages due to missing volume information.

** The non-seasalt (nss) fraction calculations assume all Cl is of marine origin and use the SO_4/Cl in seasalt ratio from Keene et al. (1986).

*** Calculations assume linear mixing of seasalt and non-seasalt sulfate

Table 4: Anion chemistry of the Guaba (tributary of Rio Icacos) and Bisley streams compared to groundwater sampled at the Icacos site. The streams were sampled at or near baseflow.

Sampling date	**Cl [μM]**	**SO_4 [μM]**	**SO_4 $\delta^{34}S$ [‰]**
Guaba stream:			
2/2/12	175	13.9	20.2
3/8/12	206	14.9	17.7
6/20/12	165	14.8	20.6
average	***182 ± 21***	***14.6 ± 0.5***	***19.5 ± 1.6***
Bisley stream:			
2/2/12	221	39.1	1.9
3/8/12	226	39.5	0.9
6/26/12	214	39.7	2.0
average	***220 ± 6***	***39.4 ± 0.3***	***1.6 ± 0.7***
*Icacos groundwater:**			
8/18/12	160	14.6	20.2

* LGW1, ~6 m deep

FIGURES CAPTIONS

Figure 1: Map of the study area, showing location of the lysimeter fields. Courtesy of Miguel Leon through the Luquillo Critical Zone Observatory (EAR-0722476).

Figure 2 a-h: Depth trends in total S, C:S, N:S and sulfate S concentration for the Icacos (a-d) and Bisley (e-h) soils. Except for the pit soils, which were sampled according to horizon designation, all other data are averages of two soil cores; error bars represent the range observed among the different core samples.

Figure 3 a-h: Soil S isotopes compared with vegetation litter and pore water averaged over the entire study period at Icacos (a-d) and Bisley (e-h). The sample at 0 cm is the O horizon. Except for the pit soils, which were sampled according to horizon designation, all other data are averages of two soil cores. Error bars for soil, pore water and vegetation litter values represent the range observed among the different soil core samples, different months, and different litter types respectively.

Figure 4 a-d: Depth trends in pore water sulfate concentration and $\delta^{34}S$ values averaged over the entire sample period at the Icacos (a-b) and Bisley (c-d) sites. The error bars are standard deviations. Vertical lines represent the sulfate concentration or $\delta^{34}S$ values of volume-weighed average precipitation (AP), groundwater (GW) at the Icacos site, Guaba baseflow (GB) and Bisley baseflow (BB).

Figure 5 a-f: The fate of atmospheric S in the soils at Icacos (a-c) and Bisley (d-f). Arrows shown represent fluxes in and out of the pore water (not the bulk soil). Solid arrows represent fluxes of sulfate, dashed arrows represent fluxes of other S compounds (e.g. organic S from litterfall and reduced S gases). S in litterfall was calculated using mean litterfall values from Weaver and Murphy (1990) and Zou et al. (1995). S in vegetation uses aboveground biomass estimates from Gould et al. (2006). The hydrologic export calculations use average runoff estimates for the Guaba and Bisley streams from Stallard and Murphy (2012) and Schellekens et al. (2004) respectively. Hydraulic field flux densities for calculating downward S fluxes in pore water are from Buss et al. (2011).

Figure 6 a-d: δ values versus the natural logarithm of concentration for N and S at Icacos (a-b) and Bisley (c-d). Only significant linear regressions are shown.

Figure 1

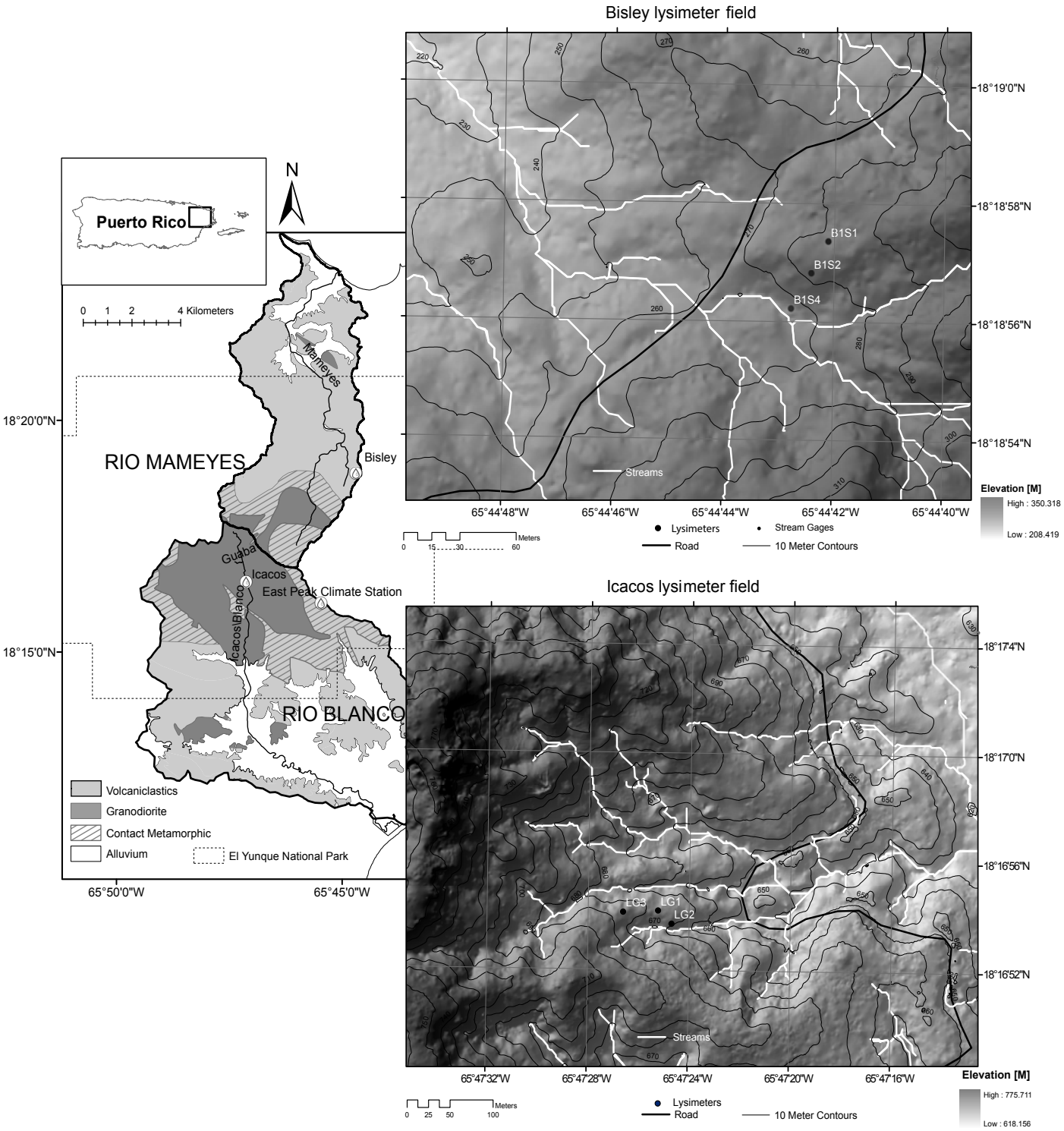
Bisley lysimeter field
Puerto Rico
N
0 1 2 4 Kilometers
Mameyes
RIO MAMEYES
Bisley
Guaba
Icacos
East Peak Climate Station
Icacos Blanco
RIO BLANCO
18°20'0"N
18°15'0"N
65°50'0"W
65°45'0"W
Volcaniclastics
Granodiorite
Contact Metamorphic
Alluvium
El Yunque National Park
B1S1
B1S2
B1S4
Streams
18°19'0"N
18°18'58"N
18°18'56"N
18°18'54"N
65°44'48"W
65°44'46"W
65°44'44"W
65°44'42"W
65°44'40"W
Meters
0 15 30 60
Lysimeters
Stream Gages
Road
10 Meter Contours
Elevation [M]
High : 350.318
Low : 208.419
Icacos lysimeter field
LG3
LG1
LG2
Streams
18°17'4"N
18°17'0"N
18°16'56"N
18°16'52"N
65°47'32"W
65°47'28"W
65°47'24"W
65°47'20"W
65°47'16"W
Meters
0 25 50 100
Lysimeters
Road
10 Meter Contours
Elevation [M]
High : 775.711
Low : 618.156

Figure 2

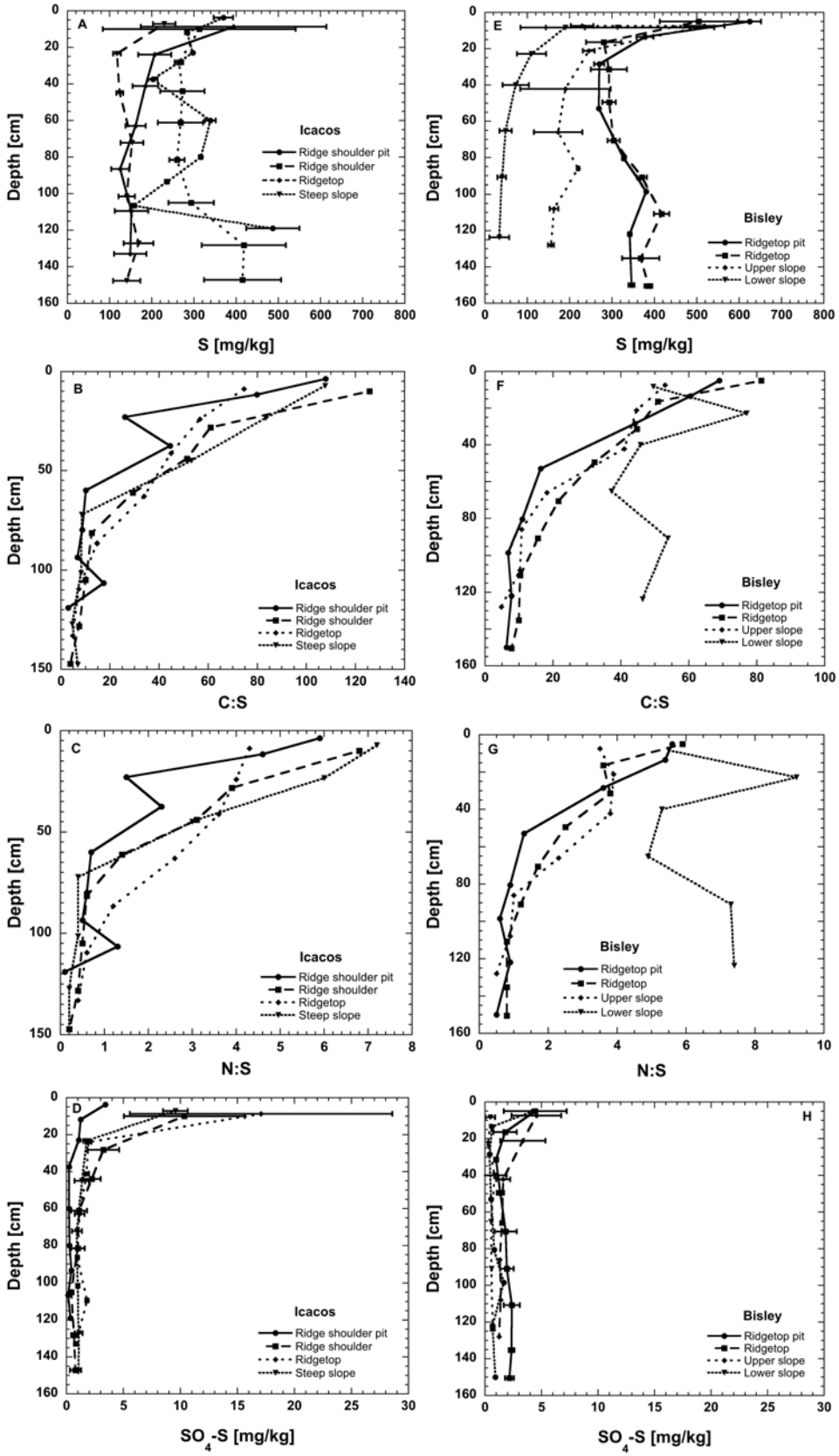
A
Icacos
Ridge shoulder pit
Ridge shoulder
Ridgetop
Steep slope
Depth [cm]
S [mg/kg]
E
Bisley
Ridgetop pit
Ridgetop
Upper slope
Lower slope
B
C:S
F
C
N:S
G
D
SO4-S [mg/kg]
H

Figure 3

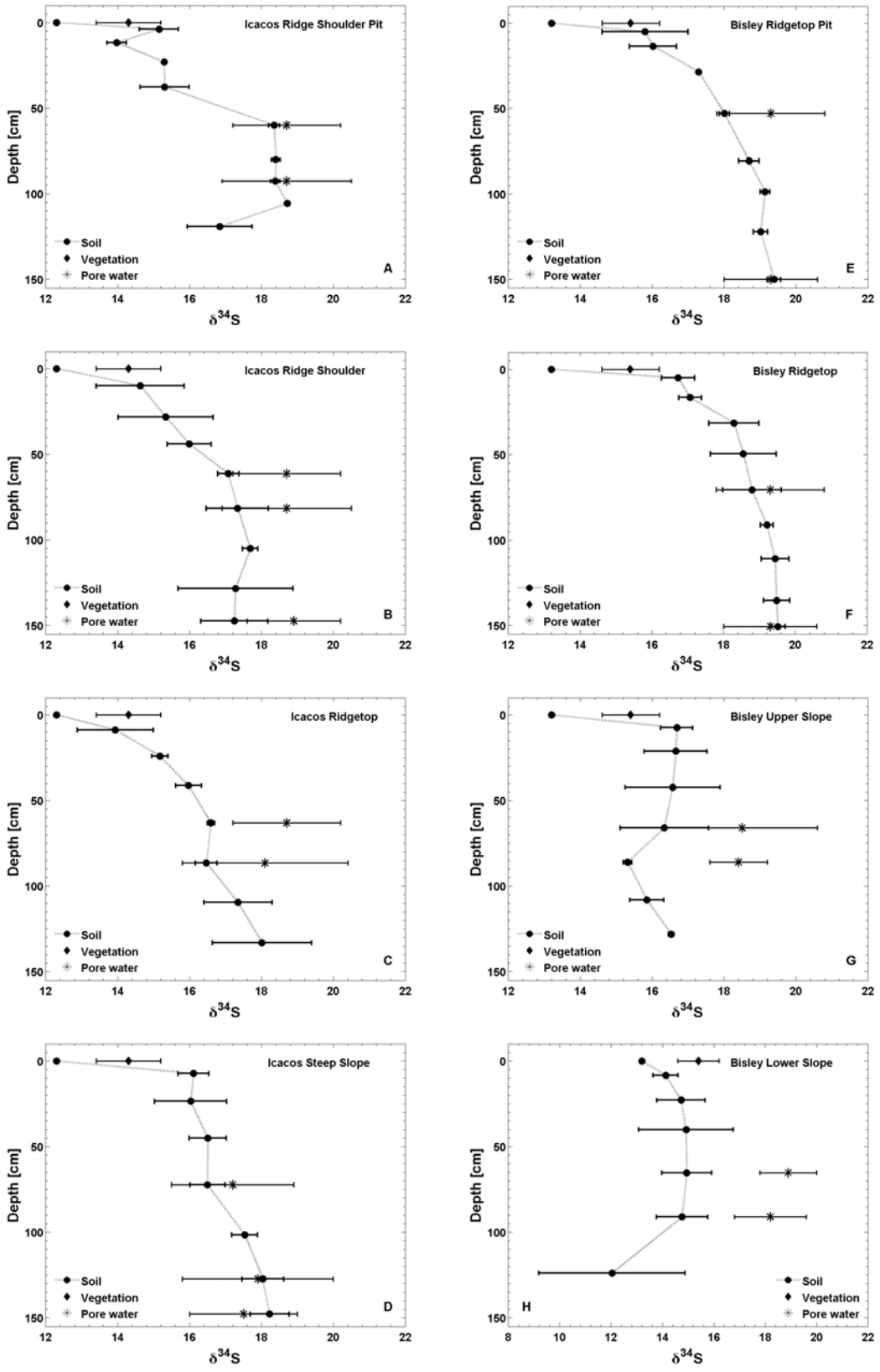
Icacos Ridge Shoulder Pit
A
Bisley Ridgetop Pit
E
Icacos Ridge Shoulder
B
Bisley Ridgetop
F
Icacos Ridgetop
C
Bisley Upper Slope
G
Icacos Steep Slope
D
Bisley Lower Slope
H
Soil
Vegetation
Pore water
Depth [cm]
δ34S

Figure 4

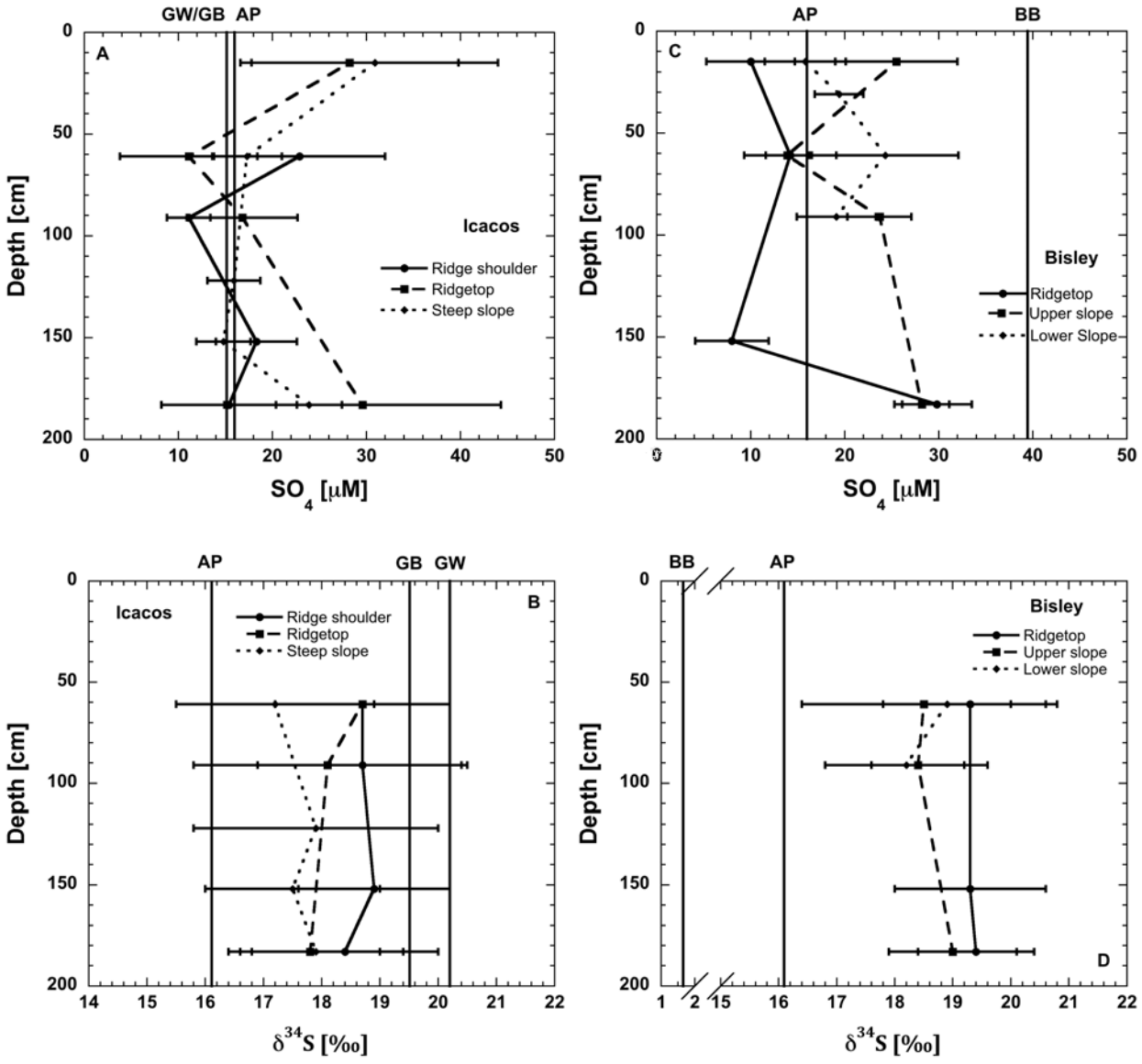
GW/GB AP
A
Icacos
Ridge shoulder
Ridgetop
Steep slope
Depth [cm]
SO4 [μM]
AP BB
C
Bisley
Ridgetop
Upper slope
Lower Slope
AP GB GW
B
Icacos
Ridge shoulder
Ridgetop
Steep slope
δ34S [‰]
BB AP
Bisley
Ridgetop
Upper slope
Lower slope
D

Figure 5

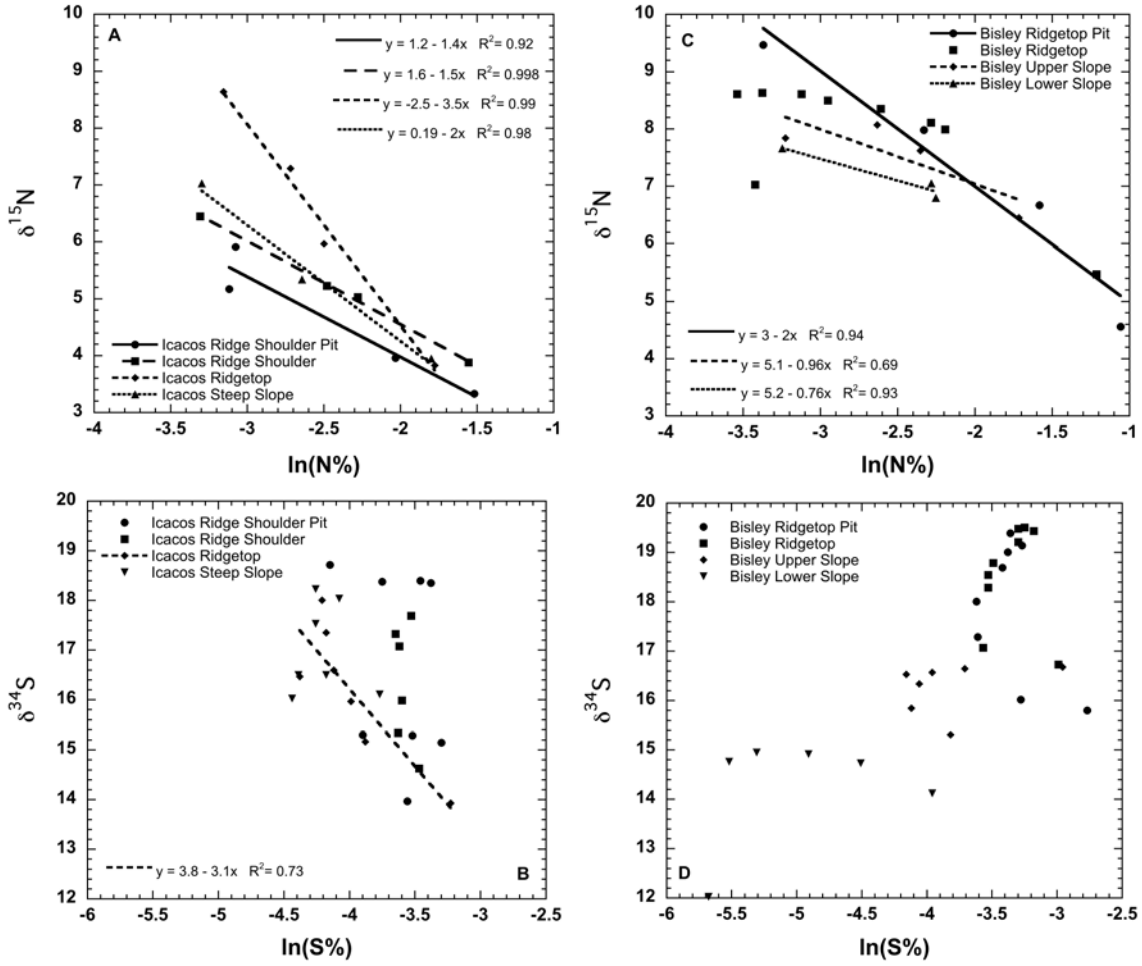
A
y = 1.2 - 1.4x R²= 0.92
y = 1.6 - 1.5x R²= 0.998
y = -2.5 - 3.5x R²= 0.99
y = 0.19 - 2x R²= 0.98
Icacos Ridge Shoulder Pit
Icacos Ridge Shoulder
Icacos Ridgetop
Icacos Steep Slope
δ15N
ln(N%)
C
Bisley Ridgetop Pit
Bisley Ridgetop
Bisley Upper Slope
Bisley Lower Slope
y = 3 - 2x R²= 0.94
y = 5.1 - 0.96x R²= 0.69
y = 5.2 - 0.76x R²= 0.93
δ15N
ln(N%)
Icacos Ridge Shoulder Pit
Icacos Ridge Shoulder
Icacos Ridgetop
Icacos Steep Slope
y = 3.8 - 3.1x R²= 0.73
B
δ34S
ln(S%)
Bisley Ridgetop Pit
Bisley Ridgetop
Bisley Upper Slope
Bisley Lower Slope
D
δ34S
ln(S%)

Figure 6

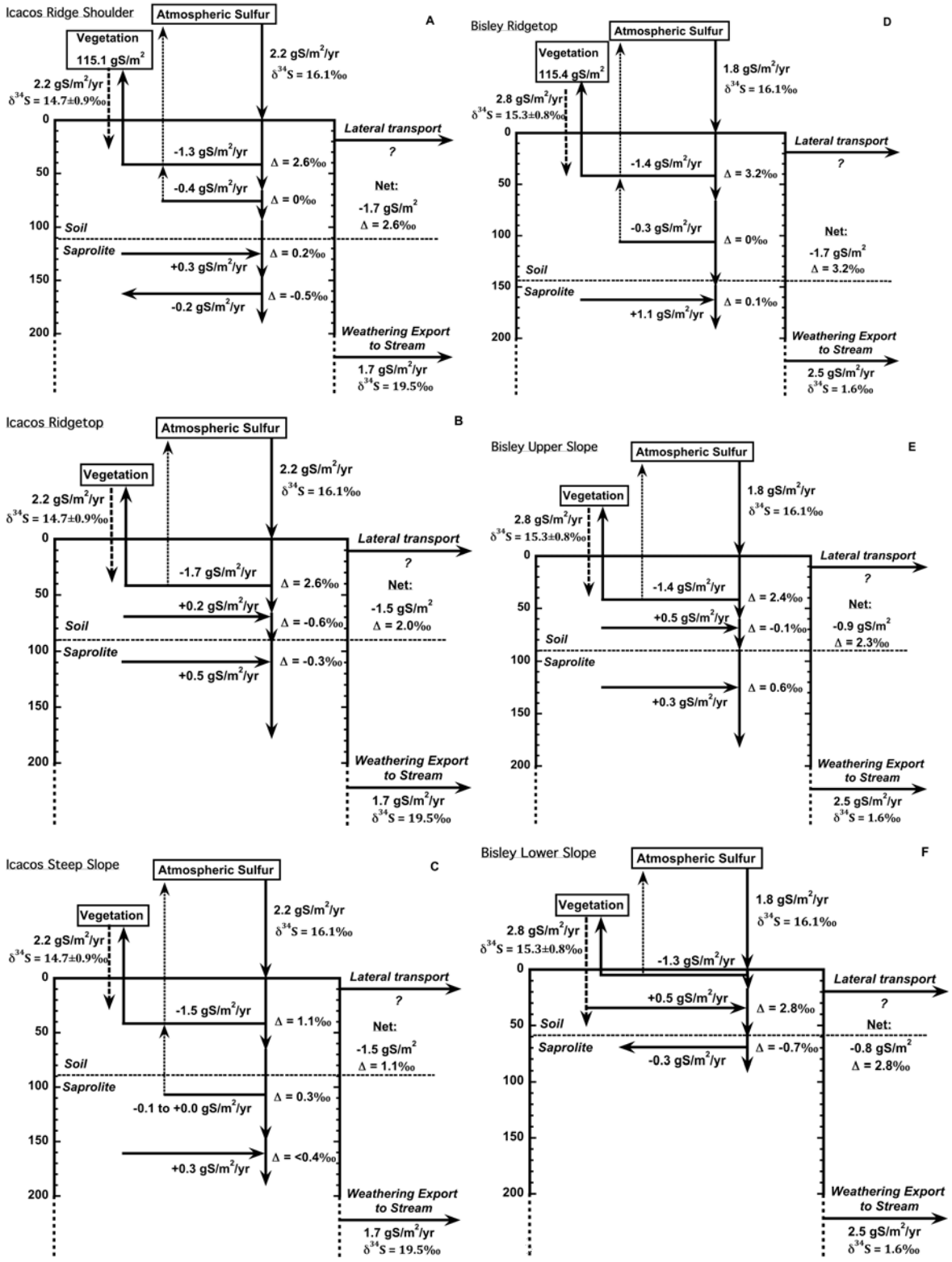
Icacos Ridge Shoulder
A
Atmospheric Sulfur
Vegetation
115.1 gS/m2
2.2 gS/m2/yr
δ34S = 14.7±0.9‰
2.2 gS/m2/yr
δ34S = 16.1‰
Lateral transport
?
-1.3 gS/m2/yr
Δ = 2.6‰
-0.4 gS/m2/yr
Δ = 0‰
Net:
-1.7 gS/m2
Δ = 2.6‰
Soil
Saprolite
+0.3 gS/m2/yr
Δ = 0.2‰
Δ = -0.5‰
-0.2 gS/m2/yr
Weathering Export to Stream
1.7 gS/m2/yr
δ34S = 19.5‰
Icacos Ridgetop
B
Atmospheric Sulfur
Vegetation
2.2 gS/m2/yr
δ34S = 14.7±0.9‰
2.2 gS/m2/yr
δ34S = 16.1‰
Lateral transport
?
-1.7 gS/m2/yr
Δ = 2.6‰
Net:
-1.5 gS/m2
Δ = 2.0‰
+0.2 gS/m2/yr
Δ = -0.6‰
Soil
Saprolite
+0.5 gS/m2/yr
Δ = -0.3‰
Weathering Export to Stream
1.7 gS/m2/yr
δ34S = 19.5‰
Icacos Steep Slope
C
Atmospheric Sulfur
Vegetation
2.2 gS/m2/yr
δ34S = 14.7±0.9‰
2.2 gS/m2/yr
δ34S = 16.1‰
Lateral transport
?
-1.5 gS/m2/yr
Δ = 1.1‰
Net:
-1.5 gS/m2
Δ = 1.1‰
Soil
Saprolite
-0.1 to +0.0 gS/m2/yr
Δ = 0.3‰
Δ = <0.4‰
+0.3 gS/m2/yr
Weathering Export to Stream
1.7 gS/m2/yr
δ34S = 19.5‰
Bisley Ridgetop
D
Atmospheric Sulfur
Vegetation
115.4 gS/m2
1.8 gS/m2/yr
δ34S = 16.1‰
2.8 gS/m2/yr
δ34S = 15.3±0.8‰
Lateral transport
?
-1.4 gS/m2/yr
Δ = 3.2‰
-0.3 gS/m2/yr
Δ = 0‰
Net:
-1.7 gS/m2
Δ = 3.2‰
Soil
Saprolite
+1.1 gS/m2/yr
Δ = 0.1‰
Weathering Export to Stream
2.5 gS/m2/yr
δ34S = 1.6‰
Bisley Upper Slope
E
Atmospheric Sulfur
Vegetation
1.8 gS/m2/yr
δ34S = 16.1‰
2.8 gS/m2/yr
δ34S = 15.3±0.8‰
Lateral transport
?
-1.4 gS/m2/yr
Δ = 2.4‰
Net:
-0.9 gS/m2
Δ = 2.3‰
+0.5 gS/m2/yr
Δ = -0.1‰
Soil
Saprolite
+0.3 gS/m2/yr
Δ = 0.6‰
Weathering Export to Stream
2.5 gS/m2/yr
δ34S = 1.6‰
Bisley Lower Slope
F
Atmospheric Sulfur
Vegetation
1.8 gS/m2/yr
δ34S = 16.1‰
2.8 gS/m2/yr
δ34S = 15.3±0.8‰
-1.3 gS/m2/yr
Lateral transport
?
+0.5 gS/m2/yr
Δ = 2.8‰
Net:
-0.8 gS/m2
Δ = 2.8‰
Soil
Saprolite
-0.3 gS/m2/yr
Δ = -0.7‰
Weathering Export to Stream
2.5 gS/m2/yr
δ34S = 1.6‰
0
50
100
150
200

Appendix

Click here to download Appendix: Yi-Balan et al_Appendix_Revised.doc